HYPERPHOSPHORYLATION AND MUTATION ENHANCE TAU AGGREGATION

DISSERTATION

Presented in Partial Fulfillment of the Requirements for the Degree Doctor of Philosophy in the Graduate School of the Ohio State University

By

Qi Zhong, M.S.

*****

The Ohio State University

2008

Dissertation Committee:

Jeff Kuret, PhD, Adviser

Mike Zhu, PhD

Glen Lin, PhD

Chen Gu, PhD

Approved by

_____

Adviser

Neuroscience Graduate Studies Program

ABSTRACT

Tauopathies refer to a diverse set of sporadic and familial neurodegenerative disorders including Alzheimer's disease (AD), and frontotemporal dementia with Parkinsonism linked to chromosome 17 (FTDP-17). All of these diseases have the formation of filamentous inclusions in both neurons and glia, which are composed primarily of hyperphosphorylated tau protein. The severity of the diseases appears to correlate with the extent of filamentous tau deposition. Understanding the mechanism under which tau fibrillizes has important implications for clarifying the pathogenesis of tauopathies.

Casein kinas 1 (CK1) family is serine/theronine specific protein kinases and they are highly associated with AD brain-derived tau filaments and granulovacuolar bodies, which are one of the hallmarks of AD and appear primarily within the hippocampus. At least six CK1 isoforms (CK1-α, γ1, γ2, γ3, δ, ε) are known to exist in human central nervous system. Real time RT-PCR was used to quantify the relative mRNA expression levels of CK1 isoforms in AD and non-AD control cases. Our data showed that of CK1-δ had 13-fold increase and CK1-γ2 had 4-fold increase in AD cases compared to control case. The rest of CK1 isoforms (CK1-α, γ1, γ3, ε) showed no statistical

difference between AD and control groups. In conclusion, increased CK1-δ and CK1-γ2 mRNA levels in postmortem AD hippocampus indicate that CK1-δ and CK1-γ2 might be candidate kinases involving in the hyperphosphorylation of tau in AD.

Recent genetic analysis has established a clear cause and effect relationship between tau gene intronic mutations and the autosomal dominant dementia in FTDP-17. These intronic mutations produce normal tau protein, but the 4R/3R isoform ratio is elevated. Since tau assembles via a nucleation dependent mechanism, using quantitative electron microscopy, the nucleation kinetics for 3R and 4R tau isoforms were assessed through the collection of critical concentrations and time courses. Our results show that 4R tau isoforms require much lower critical concentrations and possess higher nucleation efficiency than 3R tau isoforms. The dominant performance in fibrillization of 4R isoforms over 3R isoforms is accredited to the relative efficiency of exons 2, 3 and 10 in promoting tau monomer aggregation. Quantitative analysis demonstrates that exon 10 is a much stronger driving force to filament formation than exons 2, and 3.

In summary, hyperphosphorylation of tau by CK1 isoforms and increased exon 10 splice-in contribute to the aggregation of tau. Thus, CK1 isoforms and 4R tau isoforms may be valuable therapeutic targets for AD and other tauopatheis.

DEDICATION

Dedicated to my parents, grandparents, my husband and my son.

ACKNOWLEDGMENTS

First, I would like to acknowledge my advisor Dr. Jeff Kuret who has always been supportive, helpful and patient throughout my time in the lab. Without his guidance and support, I would not be able to accomplish my doctoral degree.

Also I would like to thank my former lab mates. Dr. Erin Congdon helped with the project on the time courses for four tau isoforms. I would also like to thank all of my other former lab mates. They are Drs. Haishan Yin, Guibin Li, Theresa Kannanayakal, Carmen Chirita, and Mihaela Necula. They are also authors of my two review papers. In addition, I would also like to thank our former lab technician Kelly Laguna for teaching me genetic cloning techniques.

I would like to thank my committee members Dr. Mike Zhu, Dr. Glen Lin, and Dr. Chen Gu for their teaching and suggestions while writing this thesis.

Finally, I would like to acknowledge my parents and my husband who have provided huge support and encouragement throughout my graduate education. And I also want to thank my twenty-two-month old son. He has made my life more joyful and meaningful.

VITA

1978……Born, China

1996-2001…..…Bachelor of Clinical Medicine
Hunan Medical University, China

9/2007-12/2007……...Master of Biophysics
the Ohio State University

9/2001-9/2005, 9/2007-present……..Graduate Research Associate,
the Ohio State University

PUBLICATIONS

Kuret J, Chirita CN, Congdon EE, Li G, Necula M, Yin H, **Zhong Q** (2005) Pathways of tau fibrillization. *Biochim Biophys Acta*. **1739**:167-78

Kuret J, Congdon EE, Li G, Yin H, Yu X, **Zhong Q** (2005) Evaluating triggers and enhancers of tau fibrillization. *Microsc Res Tech.* **67**:141-55

FIELD OF STUDY

Major Field: Neuroscience

TABLE OF CONTENTS

LIST OF TABLES

LIST OF FIGURES

LIST OF ABBREVIATIONS

3R, three microtubule repeat containing isoform; 4R, four microtubule repeat containing isoform; AA, arachidonic acid; AD, Alzheimer's disease; ALS, amyotrophic lateral sclerosis; ANS, 8-anilino-1-naphthalenesulfonic acid; CBD, corticobasal degeneration; CC, critical concentration; CR, Congo Red; DMSO, dimethylsulfoxide; DTT, dithiothreitol; EM, electron microscopy; FTDP, frontotemporal dementia with Parkinsonism; FTDP-17, frontotemporal dementia with Parkinsonism associated with chromosome 17; FTLD, frontotemporal lobar degeneration, formerly Pick's disease; h, hours; K_{crit}, critical concentration; k_{app}, apparent rate constant; k_{off}, reverse elongation constant; k_{on}, forward elongation constant; LLS, laser light scattering; μM, micromolar; mM, millimolar; nm, nanometer; nM, nanomolar; PHF, paired helical filament; s, seconds; STEM, scanning transmission electron microscopy; TEM, transmission electron microscopy; PSP, progressive supranuclear palsy; ThS, thioflavin S; TR, thiazine red: C_T, Threshold cycle numbers; CK1, casein kinase 1; ng, nanogram; RT-PCR, reserse trancriptase polymerize chain reaction; DS, Down syndrome; PDC, parkinsonism dementia complex of Guam; PiD, Pick's disease; PPND, pallido-ponto-nigral degeneration; PD, Parkinson's disease; DLB, dementia with Lewy bodies; ALS, amyotrophic lateral sclerosis; GAPDH, glyceraldehyde-3-phosphate dehydrogenase; PP2A, protein phosphatase 2A.

CHAPTER 1

1 INTRODUCTION

1.1 Tau protein

1.1.1 Alternative mRNA splicing forms six tau isoforms

The family of tau isoforms is composed by a set of molecular species that share common peptide sequences. There is a single gene that contains several exons encoding for the six different tau isoforms in human brain **(Figure 1.1**). The tau gene is located on the long arm of chromosome 17 and consists of 16 exons. Eleven of the exons are translated to form tau protein in adult brain. Tau discharges its functions by producing multiple isoforms via intricately regulated alternative splicing (Sisodia and Tanzi 2007). Tau isoforms generated by alternative splicing differ from one another by having either three or four microtubule binding repeats in their C-terminal half and having a variable number of inserts in their N-terminal moiety. These repeats have been shown to constitute microtubule binding motifs (Liu and Gong 2008). Exons 2, 3, 10 are alternatively spliced, leading to the presence of six different tau isoforms ranging from 352 to 441 amino acids (Hernandez and Avila 2007). All of the six isoforms have at least three microtubule binding domains encoded by exons 9, 11, and 12. In addition, exon 10 encodes an extra microtubule binding domain. Based on the presence or absence of this extra microtubule binding domain encoded by exon 10, tau isoforms can

be divided into two groups and each group have three isoforms members: the three-repeat (3R) tau and the four-repeat (4R) tau (Avila 2007). All tau isoforms share a conserved carboxyl-terminal domain containing the microtubule binding repeats (3R or 4R) and an amino terminal projection domain of varying size (Abeliovich, Schmitz et al. 2000; Dehmelt and Halpain 2005). These isoforms modulate tau function in normal brain by altering the domains of the protein, and hence modulate their affinity for microtubules and other ligands (Levy, Leboeuf et al. 2005).

1.1.2 Nomenclature of tau isoforms

The nomenclature used here for the six isoforms is based on the alternative splicing of exons 2, 3 and 10 **(Table1.1).** Among the six isoforms, exon 2 can appear alone, but exon 3 never appears independent of exon 2. The names from the longest to the shortest isoforms are respectively: N2R4, N1R4, N0R4, N2R3, N1R3, N0R3. This nomenclature clearly demonstrates the alternative splicing of the three exons: where "N*" indicates the N-terminal, the number "2" means there are exons 2 and 3 in the N-terminal of this isoform; number "1" means there is only exon 2 and "0" means there are neither of exon 2 nor 3 in the N-terminal. R3 or R4 indicates the exon 10-skipping three- repeat or the exon 10-containing four-repeat isoforms (Liu and Gong 2008).

1.1.3 Differential expression of tau isoforms

Tau isoforms are expressed in a stage- and cell type-specific manner. Tau isoforms are differentially expressed during early development. The shortest isoform N0R3,

without the two N-terminal inserts and with only three microtubule binding domains, is predominantly expressed in the fetal brain and during the first days of postnatal development. While six isoforms are all expressed during adulthood (Kosik, Orecchio et al. 1989). The switch in RNA splicing after birth to produce adult tau isoforms indicates that each of these isoforms is likely to have particular physiological roles. Recent studies have shown that tau isoforms are likely to have specific functions related to the presence or absence of regions encoded by exons 2, 3, and 10. Exons 2 and 3 modulate interactions with the axonal membrane. Exon 10 increases affinity to microtubules and may be important in the transition from the more fluid fetal cytoskeleton to the more stable adult one (Andreadis 2005).

1.1.4 Physiological and pathological roles for tau protein

Tau protein is mainly expressed in neurons and is a neuronal microtubule-associated protein (MAP), which localizes primarily in the axon (Samsonov, Yu et al. 2004). It is one of the major and most widely distributed MAPs in the central nervous system (Dehmelt and Halpain 2005). In neurons, a specific axonal compartmentalization of tau has been shown (DiTella, Feiguin et al. 1994). The distribution of tau mRNA is abundant throughout the neuronal soma and into the proximal parts of dendrites of neurons in cerebral cortex and hippocampus (Paglini, Peris et al. 2000). Even neurons containing neurofibrillary tangles continue to synthesize tau protein (Yasojima, McGeer et al. 1999). In nerve cells immunohistochemistry shows complementary distributions, with tau being concentrated in axons and high molecular mass MAP2 being confined to

dendrites. However, studies also demonstrate that tau displays a widespread distribution in a variety of non-neuronal cell types such as glial cells (Takeda, Arai et al. 1997).

Tau is first discovered as a microtubule-associated protein and its main known physiological function is to regulate the dynamics of the microtubule network, especially involving in the axonal transport and neuronal plasticity (Avila 2004). Being an important component of microtubules, tau is essential for establishing neuronal cell polarity and axonal outgrowth during development, and for maintaining axonal morphology and axonal transport in matured cells (Buee, Bussiere et al. 2000; Paglini, Peris et al. 2000; Feinstein and Wilson 2005). Tau binds directly to microtubules and regulates their growing and shortening dynamics (Feinstein and Wilson 2005). Microtubules exhibit dynamic instability and its intrinsic behavior is characterized by alternating phases of growth, shortening, and pausing. Transitions between the growth and shortening states are called catastrophes and rescues. Tau binds along the length of microtubules and stabilizes microtubules by reducing catastrophe and promoting rescue frequencies, leading to prolonged growth periods and thus enhanced net microtubule accumulation (Dehmelt and Halpain 2004). Tau can also increase microtubule rigidity and induce microtubule bundles in heterogeneous cell systems (Dehmelt and Halpain 2005). Tau knock out studies showed that tau played a specific, but nonessential, role in the morphogenesis of the nervous system. It probably has multiple other roles in other pathways and can be compensated for by other proteins with redundant functions (Dehmelt and Halpain 2005).

On the other hand, cells exert powerful regulation over tau activity via two main mechanisms: First, alternative splicing leads to the expression of two classes of tau proteins, the more potent 4R tau isoform and the less potent 3R isoforms (Shi, Zhang et al. 2008); Second, cells also regulate tau activity via kinases and phosphatases activity upon its approximately two dozen phosphorylation sites (Buee, Bussiere et al. 2000; Feinstein and Wilson 2005).

The microtubule-associated protein tau has gained much attention due to the fact that it is deposited in cells as fibrillar lesions in numerous neurodegenerative diseases, and most notably Alzheimer's disease. Tau polymers are the prevalent species observed in aging disorders as such AD and many other neurodegenerative diseases, suggesting that this morphology of aggregation represents a significant pathological role. As a consequence of an independent insult or aging itself, the filament shifts from a physiological role to one with pathological implications. The relative importance of tau filaments has also been a focus of significant debate within the research community. Since tau pathology has been found to correlate with symptom presentation in patients, tau filaments not only greatly contribute to the pathological process of neuronal loss, but also represent a physiological process whose regulation may be controlled (King 2005).

1.2 Phosphorylation of tau

Tau plays a key role in regulating microtubule dynamics, axonal transport and neurite outgrowth, and all these functions of tau are modulated by site-specific phosphorylation. There is significant evidence that a disruption of normal

phosphorylation events results in tau dysfunction in neurodegenerative diseases. Indeed, the abnormal tau phosphorylation that occurs in neurodegenerative conditions not only results in a toxic loss of function (e.g. decreased microtubule binding) (Feinstein and Wilson 2005) but probably also a toxic gain of function (e.g. tau aggregate into filaments), as they are in the disease state, result in tau dysfunction and mislocalization, which is potentially followed by tau polymerization, neuronal dysfunction and death (Stoothoff and Johnson 2005). Although tau is phosphorylated *in vitro* by numerous protein kinases, how many of these actually phosphorylate tau *in vivo* is unclear. It is of crucial importance to identify the protein kinases and phosphatases as well as the signaling cascades that regulate tau phosphorylation *in vivo* in both physiological and pathological processes. Thus, it will also provide potential therapeutic targets for the treatment of AD and other neurodegenerative diseases.

1.2.1 Protein kinases that phosphorylate tau

Protein kinases are enzymes responsible for the phosphorylation of hydroxyl side-chains on proteins by catalyzing the transfer of a phosphate from ATP. This phosphorylation produces a change in the function of the protein concerned. Phosphorylations take place on serine, threonine and tyrosine residues and hence the enzymes are termed serine/threonine (Ser/Thr) or tyrosine kinases. In AD, perturbations to the balance of kinase and phosphatase activities may lead to the inappropriate hyperphosphorylation of various proteins (Wang, Grundke-Iqbal et al. 2007). Phosphorylated tau proteins accumulate early in neurons, even before formation of

neurofibrillary tangles, suggesting that an imbalance between the activities of protein kinases and phosphatases acting on tau is an early phenomenon (Bancher, Brunner et al. 1989) The consensus view in the literature suggests that the protein kinases most predominantly involved in AD-specific tau phosphorylation are clyclin-dependent kinase 5 (Cdk5) (Hutton, Lendon et al. 1998; Kelleher, Garwood et al. 2007; Lopes, Oliveira et al. 2007; Chen, Huang et al. 2008); glycogen synthase-3 beta (GSK-3 beta) (Mandelkow, Drewes et al. 1992; Cho and Johnson 2004; Avila and Hernandez 2007; Hooper, Killick et al. 2008); mitogen-activated protein kinases (MAP kinase) (Mandelkow, Drewes et al. 1992; Timm, Matenia et al. 2006); externally regulated kinase, (ERK1 and ERK2)(Ferrer, Blanco et al. 2001); prokein kinase A (PKA) (Khan and Alkon 2006); protein kinase C (PKC) (Hutton, Lendon et al. 1998); pk40 neurofilament kinases (Roder, Eden et al. 1993); neuronal cdc2-like kinase (Agarwal-Mawal and Paudel 2001). Recently, it has shown by immunohistochemistry that casein kinase 1 delta (CK1- delta) is associated with granulovacuolar bodies and tau containing NFTs in AD and a number of other neurodegenerative diseases (Schwab C 1995).

1.2.2 Tau dephosphorylation

Down-regulation of protein phosphatase 2A (PP2A) is thought to play a critical role in tau hyperphosphorylation in Alzheimer's disease. Findings have suggested that increased PP2A phosphorylation can consequently compromise dephosphorylation of abnormally hyperphosphorylated tau, and lead to neurofibrillary tangle formation (Liu, Zhou et al. 2008) (Liang, Liu et al. 2008). One research suggested that activation of PP-

2A or inhibition of either both GSK-3beta and cdk5 or one of these two kinases plus PKA or CaMKII might be required to inhibit Alzheimer neurofibrillary degeneration (Wang, Grundke-Iqbal et al. 2007). The role of O-GlcNAc may also offer a route to blocking pathological hyperphosphorylation of tau in AD. The reciprocal relationship between phosphorylation and O-GlcNAc modification of tau and reductions in O-GlcNAc levels on tau in AD brain offers motivation for the generation of potent inhibitors for tau hyperphosphorylation in brains (Yuzwa, Macauley et al. 2008).

1.3 Tau protein is involved in a large group of diseases called tauopathies

Proteins that fail to achieve a folded functional state, may result in the formation of deposits consisting of assembled monomeric protein, a process known as protein fibrillization(Uversky, Oldfield et al. 2008). Over 20 conformational diseases have been identified so far including Alzheimer's disease, Parkinson's disease(Selkoe 2004), and Huntington's disease (Rubinsztein and Carmichael 2003) that are a result of protein misfolding. Recently, it has been proposed that perhaps all proteins can aggregate *in vitro* into fibrils indistinguishable from observed *ex vivo* and associated to disease(Macario and Conway de Macario 2000). Without binding to microtubules, tau is natively unfolded molecules lacking secondary structure. It adopts a conformational change from random coil to beta-sheet structure upon binding to its target (Uversky 2002). The microtubule binding domains (MBDs) have been identified to be crucial for this conformational switch (Uversky 2002).

Aberrant aggregates of tau have been documented in most of the neurodegenerative diseases with filamentous inclusions. Previous studies have indicated that tau belongs to a unique group of “natively unfolded proteins” that upon binding to its target gains structure to stabilize microtubules (Wright and Dyson 1999). The MBD region has been identified as the region responsible for microtubule stabilization and also forms the core of paired helical filaments(King, Ghoshal et al. 2001). Assembled tau in these disorders assumes the appearance of paired helical filaments, straight filaments and twisted filaments (Gray, Paula-Barbosa et al. 1987). Filamentous tau differs from its normal counterpart in posttranslational modification, detergent solubility, subcellular location, and ability to bind microtubules. Tau proteins are also powerful markers of the neuronal physiological state. Their degree of phosphorylation is a good marker of cell integrity. It is heavily disturbed in numerous neurodegenerative disorders, leading to a collapse of the microtubule network and the presence of intraneuronal lesions resulting from tau aggregation (Hernandez and Avila 2007). Because tau filaments form in brain regions associated with memory retention, and because their appearance correlates well with the degree of dementia, they have emerged as robust markers of disease progression (Braak and Braak 1991; Braak, Braak et al. 1994). Thus tau filament formation heralds the onset of cytoskeleton disorganization that is characteristic of degenerating neurons and may represent a fundamental pathological response of neurons to various insults.

Filamentous tau deposits in neurons or glia cells in the absence of amyloid plaques constitute a defining characteristic of a large group of neurodegenerative diseases collectively called tauopathies (Gasparini L 2007). They includes Alzheimer’s disease

(AD) and a diverse group of disorders called the frontotemporal dementias (FTD), which are two of the most common forms of dementia and afflict more than 10% of the elderly population(Gasparini L 2007). FTD with tauopathies mainly include frontotemporal dementia and Parkinsonism linked to chromosome 17 (FTDP-17), corticobasal degeneration (CBD), progressive supranuclear palsy (PSP), Argyophilic Grain Disease (AGD) and Pick's disease. They all have filamentous inclusions composed primarily of tau, which involves the assembly of hyperphosphorylated tau into filaments and the congregation of the filaments to form inclusions. The rest of the FTD is not associated with tau protein. Instead, they are associated with ubiquitin. All of these types of tauopathies present heterogeneous as well as overlapping pathological changes and clinical symptoms (Hernandez and Avila 2007).

1.3.1 Classification of tauopathies based on tau isoform involved in neurofibrillary pathology

Tauopathies can be classified into three classes according to the types of isoform appeared in aggregation. The first class of tauopathies is caused by all six tau isoforms, they including Alzheimer’s disease and FTDP-17 (Gasparini L 2007). The second class is caused only by 4R isoforms. The vast majority of tauopathies fall into this class, like Cortical Basal Degeneration (CBD) (Wszolek, Tsuboi et al. 2006) and Progressive Suprenulear Palsy (PSP)(Ezquerra, Gaig et al. 2007), and Argyrophilic grain disease (AGD)(Ferrer, Santpere et al. 2008). The third class includes a few rarely dementia that

are entirely caused by 3R tau isoforms, like Pick's Disease (Buee, Bussiere et al. 2000; Hyman, Augustinack et al. 2005) (**Table 1.2**).

1.3.2 Tau gene deficits lead to FTDP-17

FTDP-17 is a collection of autosomal dominant tauopathies with severe frontotemporal atrophy. Although it has diverse but overlapping clinical and pathological features, its main symptoms includes behavioral and personality changes, cognitive impairment, and motor symptoms (Bancher, Brunner et al.). The prevalence and incidence of this hereditary disease remain unknown but FTDP-17 is an extremely rare condition. Since 1998, genetic studies from several groups have established a direct link between FTDP-17 disorders and mutations in the tau gene (Spillantini, Van Swieten et al. 2000). Increasing evidence clearly demonstrate that mutations in tau gene are sufficient to cause filament formation and neurodegeneration. **Figure 1.2** illustrates the possible mechanism explaining why tau gene mutations lead to disease formation. For the red arrowed boxes, the intronic and silent mutations lead to overproduction of normal 4R tau isoforms (Ingelsson, Ramasamy et al. 2007). Increased 4R tau may result in an excess of tau over available 4R binding sites on microtubules. This abundance may lead to accumulation of unassociated 4R tau. Unbound tau is phosphorylated and precipitated into filaments in neuron. Over long period of time, large amounts of toxic tau filaments form NFTs. It is well known that 4R tau possesses a greater ability to interact with microtubules than 3R tau, possibly 40-fold higher than that of 3R tau (Andreadis 2005). The excess binding with 4R tau would result in an over-rigid and

inflexible microtubule structure (Hyman, Augustinack et al. 2005). Without proper binding with proper tau isoforms, microtubules will destabilize and depolarize. This will trigger a series of abnormalities in intracellular signaling and neuronal trafficking. Neurons are unable to maintain their morphology and function and eventually undergo neuronal death. For the blue arrowed boxes, the exonic tau mutations produce normal ratio of 4R/3R tau. However, they produce abnormal tau mutants and altered tau structure leads to much reduced affinity to bind to microtubules. Without proper binding of tau, the function of microtubules is impaired as mentioned above. Excess of unbound mutant tau is precipitated to form filaments. Under similar mechanism with those intronic mutations, neurons will undergo apoptosis and over time clinic pathologic phenotype will appear.

1.3.3 Intronic and exonic FTDP-17 mutations.

Over 100 families with at least 39 different mutations in the tau gene have been identified in FTDP-17 cases worldwide (Hernandez and Avila 2007)(Gasparini L 2007) **(Figure 1.3)**. These mutations can be loosely classified into two classes. One class consists of exonic missense and deletion mutations located within the coding sequence of tau gene and influences microtubule binding. Most of these exonic mutations are located in exon 9, 10, 11, and 12. These four exons encode the four microtubule binding repeats. Not surprisingly, they reduce the affinity of tau binding to microtubules and cause MT dysfunction. The reduced affinity results in excess free mutant tau and drive aggregation and abnormal filaments formation (D'Souza and Schellenberg 2005). The

second class consists of all intronic mutations and exonic silent mutations that affect the distribution of alternatively spliced tau isoforms. They primarily affect the regulation of exon10 splicing and result in the forced splice in of exon 10 (Hernandez and Avila 2007). These intronic mutations are located at positions +3, +11, +12, +13, +14, +16 and +19 of the intron following exon 10, with the first nucleotide of the splice-donor site taken as +1. This class of mutations has no effects on tau's binding to MTs and they produce six normal tau isoforms. However, they cause exon 10 to be excessively expressed, leading to significant increase in the amount of 4R tau and raise the normal 4R/3R ratio from 1 to 2-3 (D'Souza, Poorkaj et al. 1999). Normal adult human brain expresses roughly equal amounts of 4R and 3R tau (Hutton, Lendon et al. 1998). Increased 4R isoforms have been identified in many other types of tauopathies. 4R tau mRNA was found to be elevated in AD (Yasojima, McGeer et al. 1999), PSP (Takanashi, Mori et al. 2002), CBD (Takanashi, Mori et al. 2002). Therefore, altered ratios of normal tau isoforms as well as tau mutants with altered structure clearly influence the activity and function of tau and lead directly to filament formation and neurodegeneration.

1.3.4 Significance of maintaining normal ratio of 4R/3R tau

Normal adult human brain expresses roughly equal amounts of 4R and 3R tau. However, the FTDP-17 mutations generally lead to a significant increase in the amount of 4R tau such that 4R tau comprises approximately 75% of the total while 3R tau comprises only approximately 25% (Hutton, Lendon et al. 1998) (D'Souza, Poorkaj et al.

1999). A similar situation has also been found in Alzheimer's disease. It has been shown that the exon 10 containing tau mRNA is 3.4-fold up-regulated in AD brain compared to normal brain, suggesting that tangle formation in AD is initially determined by transcriptional factors and is not exclusively by post-translational events (Yasojima, McGeer et al. 1999). So enhanced tau mRNA in AD may be a marker of attempted plasticity changes in neurodegenerative disorders. Analysis of brain tissue from a rapidly progressive frontal temporal case revealed elevated levels of exon 10 tau RNA and soluble 4R tau (Hogg, Grujic et al. 2003). Using RT-PCR and immunohistochemistry with anti-tau antibody AT8, a high yield of 4R/3R tau mRNA ratio was detected in frontal cortex and globus pallidaus of patients with progressive suprannuclear palsy and corticobasal degeneration (Takanashi, Mori et al. 2002). A recent study have demonstrated increased but largely variable 4R tau/3R tau mRNA ratios in FTLD and PSP cases (Hyman, Augustinack et al. 2005). Meanwhile, another group of scientists have shown that one of the two haplotypes of the tau gene, the H1 haplotype contains a polymorphism in the intron between exons 9 and 10, which shifts the ratio towards 4R isoforms. This haplotype in turn is associated with the development of PSP (Kowalska, Jamrozik et al. 2004). These data indicate that elevated 4R mRNA isoforms, as well as changed isoform ratio is involved in lots of different types of tauopathies (Ezquerra, Gaig et al. 2007). Therefore, maintaining a correct ratio of wild type 4R and 3R tau is essential for the normal function of tau in human brain. Skewed ratios of tau isoforms clearly influence the activity and normal function of tau and are sufficient to cause neurodegeneration.

1.4 Mechanism for tau fibrillization

Protein fibrillization is widely considered to be an assembly of misfolded or partially folded polypeptides. The main driving force behind protein fibrillization is believed to be the hydrophobic clustering of the solvent exposed hydrophobic protein regions. Other energetic factors include intermolecular electrostatic attractions and hydrogen bonding (Kuret, Congdon et al. 2005). In order for fibrillization to be thermodynamically favorable, hydrophobic regions need to be exposed to the solvent, which requires the folded structure to be destabilized. The exposure of hydrophobic regions will result in decrease of entropy in the system by ordering water molecules around the non hydrogen bonding hydrophobic regions; thus the presence of another hydrophobic region in another polypeptide will result in assembly driven by overall increase in entropy (Chirita, Necula et al. 2003). Changes in protein stability are generally attained by mutations, either sporadic or familial, protein truncations, post-translational modifications, such as glycosylation and phosphorylation, or changes in temperature, pH, ionic strength, and organic solvents (Necula and Kuret 2004). The soluble tau isoform N2R4 is one of the longest natively unfolded proteins, lacking significant amounts of secondary structure over a sequence of 441 amino acids in the longest isoform. Furthermore, the unfolded character is consistent with some notable features of the protein like stability towards heat and acid treatment. It is still unclear how these characteristics support the physiological function of binding to and stabilization of microtubules. Some recent studies on how an unfolded protein such as

tau can adopt beta-structure, which then leads to the highly ordered morphology of the paired helical filaments (PHFs) (Friedhoff, von Bergen et al. 1998). The core sequence for both microtubule binding and PHF formation is the microtubule binding domain containing three or four repeats. This region alone is sufficient for PHF formation and mostly unfolded in the soluble state. A search for sequence motifs within this region crucial for PHF building revealed two hexapeptides in the second and the third repeat. Some of the genetically linked cases of FTDP-17 show missense mutations in or adjacent to these hexapeptide motifs. Tau proteins containing the P301L and the DeltaK280 mutations exhibit accelerated aggregation (van Swieten, Bronner et al. 2007; Liu and Gong 2008). The importance of the two hexapeptides stems from their capacity to undergo a conformational change from a random coil to a beta sheet structure (von Bergen M 2005). The increase of beta sheet structure is a typical feature of an amyloidogenic protein and is the basis of other characteristics like a decreased sensitivity towards proteolytic degradation and Congo red binding. PHFs aggregated *in vitro* and *in vivo* contain beta-sheet structure, as confirmed by circular dichroism (CD) spectroscopy, Fourier transform infrared (FTIR) spectroscopy and X-ray diffraction.

1.4.1 Induce Tau fibrillization *in vitro*

Tau fibrillization *in vitro* has been widely studied for clarifying tau assembly mechanisms. Purified tau protein can form fibrillar polymers resembling the PHF found in AD brains (Hernandez and Avila 2007). However, confirming those findings *in vitro* is difficult because purified recombinant tau preparations do not aggregate

spontaneously at physiological concentrations and temperatures because of its random coil nature (King, Ahuja et al. 1999). Normal tau is a highly soluble protein under physiological conditions. The low percentage of the hydrophobic amino acids (about 15%) and the net charge at physiological pH (pI=8.3-10.0) explain the unfolded character of soluble tau protein (Uversky, Gillespie et al. 2000) (Wright and Dyson 1999). However, the addition of certain compounds highly facilitates and accelerates tau assembly. Earlier studies have shown that full-length tau protein can be induced to form tau filaments in hours by the addition of free fatty acids at 50 – 100 μ M concentration (Wilson and Binder 1997; King, Ahuja et al. 1999). Over long periods of incubation (days), straight filaments adopt paired helical morphology which is the principal form seen in late stage AD (King, Ahuja et al. 1999; King, Ghoshal et al. 2001). Many other inducers such as heparin, polyglutamate, nucleic acids, alkyl sulfate detergents, anionic microspheres have been discovered to induce the assembly of tau protein into Alzheimer-like filaments *in vitro* (Chirita, Necula et al. 2004) (Chirita and Kuret 2004) (Necula and Kuret 2004). These facilitating compounds or "inducers" can be devided into these classes: The polyanions (heparin, polyglutamate, or RNA) and free fatty acids (arachidonic acid, surfactant detergent). In addition, planar aromatic dyes, such as Thioflavin S (Necula, Chirita et al. 2005), Congo red (Li, Yin et al. 2004) and thiazine red (Yin and Kuret 2006), have been reported to enhance the tau aggregation in a certain concentration range. This work has produced a number of methods for the assembly of full-length tau into filaments *in vitro* (Chirita, Congdon et al. 2005) (Chirita, Congdon et al. 2005).

The mechanism by which these inducers help to get a filamentous state of tau protein is not clear so far. It has been proposed that the clustering of the negative charges on the inducers plays an important role. The polyanionic compounds could provide a substrate similar to the surface of microtubules, with which tau has strong interactions (Chirita, Necula et al. 2003). The fatty acids form micelles (Chirita, Necula et al. 2003), which can constitute a polyanionic cluster. The interaction of tau with clusters of negative charges could induce a conformational change from a random coil to filamentous structures (Friedhoff, Schneider et al. 1998).

Different inducers have different effects on tau fibrillization in terms of incubation time needed, substrate concentration, and final filament morphology. This indicates that inducers act differently in facilitating tau aggregation. Heparin induces tau aggregation through the formation of tau dimers (the intermolecular cross-linking of cysteine322). The advantages of heparin lie that it can induce filaments of PHF morphology. So it can be successfully used to measured structural change in tau aggregation. However, the time required to reach steady-state level is long (twenty-four hours to two weeks depending on the length of tau) and unphysiologically high tau concentration is needed. The deleted region out of the microtubule-binding repeats cannot be easily modeled (Necula, Chirita et al. 2003).

The use of free fatty acid overcomes the time and concentration limitations of heparin. Fatty acids and alkyl sulfate detergents act in micellar form and provide an anionic surfaces for tau fibrillization (Necula, Chirita et al. 2003) (Chirita, Necula et al. 2003). They promote tau fibrillization more efficiently under near physiological

conditions using physical level of tau protein concentration (Wilson and Binder 1997). It shows a high efficacy for promoting the polymerization of full-length tau at physiological concentrations (1-10 μ M) much more rapidly than heparin (Barghorn and Mandelkow 2002). Although the morphology of arachidonic acid induction is straight filament, it's similar with paired helical filament since antibodies recognize the filaments and fluorescent dyes that react with real and induced PHFs. Moreover, unlike heparin or RNA, which is sequestered from tau protein *in vivo* and couldn't act as an *in vivo* inducers, anionic micelles mimic cellular membranes which could provide intracellular anionic surfaces (Necula, Chirita et al. 2003). Thus they have been used widely for studying tau assembly pathway *in vitro*.

1.4.2 Experimental methods used for the study of tau fibrillization *in vitro*

Several methods have been used to measure tau aggregation mechanism *in vitro*: quantitive electron microscopy (Necula and Kuret 2004), fluorescence spectroscopy (Friedhoff, Schneider et al. 1998) (King, Ahuja et al. 1999), static light scattering (Necula and Kuret 2004b), sedimentation (Necula, Chirita et al. 2003), and intrinsic tau fluorescence assays (Luo, He et al. 2000). Each method has its own advantages and disadvantages and can be chosen according to proper experimental purposes.

The transmission electron microscopy (TEM) assays basically detect the filaments only after adsorption onto the hydrophobic surface of grids coated with formvar (a polyvinyl formal polymer) and carbon. Utility of this method had been debated owing to the numerous variables; however, it has been studied in great detail. Advantages of EM

includes: 1) TEM measures the filamentous tau but can exclude assembly intermediates and other non-filamentous components. 2) EM method yields the linear filaments, which are similar with authentic one from brain. 3) The unique advantage of the EM method is its ability to get morphology and length distribution information, which are essential for quantification. The EM method also has some weakness. First, this method is not universally applicable to all aggregating proteins. For example, α - synuclein can be detected as dense networks of highly curved filaments instead of separate linear filaments. Moreover, the filaments induced by heparin clump together and are hard to quantify. In addition, tau incubated at high concentrations can form aggregates termed fractals, which are characterized by irregular shapes that are recapitulated at any scale magnification. Another problem is that EM assays also share a weakness with the fluorescence assays: the lack of internal standard for converting measurements into units of mass or molar concentration. Last, the tau protein concentration competes with filaments for adsorption onto grid surface. However, dilution the sample will help to avoid such interference (Necula and Kuret 2004a).

Compared to the TEM method, solution-based methods are more rapid and straightforward. Thioflavin S is a dye that it has been traditionally applied in the examination of AD brains and also has been employed in the tau polymerization study *in vitro* by some groups (Friedhoff, Schneider et al. 1998). Now fluorescence assays are widely in used solution based methods. Thioflavin dyes are small anionic planar molecules. They exhibit fluorescence increases in the 480-520 nm wavelength at the present of β –sheet structures. The advantages of this method are very fast and can

monitor tau polymerization in real time (Chirita and Kuret 2004). But there is a very important disadvantage. ThS shows a large fluorescence increase in the presence of tau and arachidonic acid even when no filaments can be observed by electron microscopy(Barghorn and Mandelkow 2002). This indicates that a tau intermediate is formed. ThS reacts with tau this intermediates as well as mature filaments (Chirita and Kuret 2004).

Laser light scattering (LLS) is another solution-based method for studying polymerization in vitro. The underlying principle of this method is that the amount of scattered light is directly proportional to the mass of tau filaments in suspension. [50]. The filament length distribution is limited within a certain range. Because *in vitro* polymerization need to add inducers in the reaction, LLS can not be used to quantify tau polymerization using fluorescent dyes such as Thiazine red as inducers. Also, some inducers are common to form micelles, which may cause a potentially larger light scattering complex with tau and exhibit light scattering properties. Thus, this initial complex should be corrected by running a negative control consisting of assembly incompetent tau protein in parallel with the experimental sample and subtracting the two results (Necula and Kuret 2004b). In short, this method is fast and well suited for time course experiments but requires corrections for the addition of anionic inducers.

1.4.3 Tau fibrillization pathway and kinetics

Protein fibrillization is widely considered to be an assembly of misfolded or partially folded polypeptides (Etienne, Edwin et al. 2007). The main driving force

behind protein fibrillization is believed to be the hydrophobic clustering of the solvent exposed hydrophobic protein regions. Other energetic factors include intermolecular electrostatic attractions and hydrogen bonding (Kuret, Chirita et al. 2005). In order for fibrillization to be thermodynamically favorable, hydrophobic regions need to be exposed to the solvent, which requires the folded structure to be destabilized. The exposure of hydrophobic regions will result in decrease of entropy in the system by ordering water molecules around the non hydrogen bonding hydrophobic regions; thus the presence of another hydrophobic region in another polypeptide will result in assembly driven by overall increase in entropy(Gales, Cortes et al. 2005). Changes in protein stability are generally attained by mutations, either sporadic or familial, protein truncations, post-translational modifications, such as glycosylation and phosphorylation, or changes in temperature, pH, ionic strength, and organic solvents (Chirita and Kuret 2004).

Tau fibrillization pathway follows the nucleation-elongation model involving a significant conformational change and the adoption of secondary structures (Friedhoff, von Bergen et al. 1998; King, Ahuja et al. 1999). The nucleation-dependent model for protein fibrillization dictates that aggregation is dependent on protein concentration and time. In the fibrillization process, the thermodynamic effects are on solubility, stability, or structure. The kinetic effect is on rate. The kinetics of nucleation-dependent polymerization is characterized by two important factors: critical concentration and elongation lag time. These two factors symbolize the fibrillization efficiency of a certain protein monomer and provide very good substrates for analyzing tau fibrillization *in*

vitro. In a typical nucleation-dependent polymerization, polymer is not observed until the monomer concentration exceeds a certain level known as the critical concentration (CC). Critical concentration equals the number of monomers in solution at equilibrium and reflects the thermodynamic characteristic of tau fibrillization.

The time course of fibrillization is composed of three phases: a lag time phase, a growth phase, and a steady state phase (**Figure 1.4**). During the lag time phase, no filament can be detected. The lag time reflects the nucleation rate and thus the kinetic characteristic of fibrillization. The processes are characterized by a slow nucleation phase, in which the protein undergoes a series of unfavorable association steps to form an ordered oligomeric nucleus. Shorter lag time indicates faster nucleation rate. In growth phase, the nucleus rapidly grows to form larger polymers. In steady state phase, the ordered aggregates and the monomer appear to be at equilibrium.

In Summary, the characteristic features of a simple nucleation-dependent polymerization are as follows: a. No aggregation occurs at a protein concentration below the critical concentration. b. At protein concentrations that exceed the critical concentrations by a small amount, there is a lag time before polymerization occurs. c. During the lag time, addition of a seed results in immediate polymerization (Harper and Lansbury 1997). This model is widely used to study protein fibrillization pathways including tau, a-synuclein, actin, tubulin and so on.

Let's take a close look of tau fibrillization in particular (**Figure 1.5**). Whatever inducers are used, tau *in vitro* aggregation pathway is quite similar and its progression follows a sigmoidal curve. There are three major steps in tau polymerization *in vitro.*

First, natively unfolded monomer (Ux), which is assembly –incompetent, changes to an assembly-competent conformation (Uc) through triggering activity such as adding anionic inducers. Triggering activity results in a much accelerated nucleation rate. The assembly-competent conformation (intermediate) is characterized as a partially folded tau molecule enriched with β -sheet structures (Chirita and Kuret 2004).

Second, once the intermediates are populated, the reaction follows by nucleation, which is characterized by lag time and critical concentration. In this step, tau monomer associates with each other and forms "nucleus" (N). This reaction is energetically unfavorable, and is the rate-limiting step for the whole procedure. A minimum (critical) concentration of tau is required for nucleation reaction. Critical concentrations vary by each inducer added due to different inducer facilitating potency. So by applying different potent inducers, we obtain different results of critical concentrations for the same protein. The more potent the inducer is the smaller critical concentration we obtain. Similarly, by applying the same inducer, different potent proteins require different critical concentrations to start aggregation. Lower CC represents higher polymerization propensity.

Third, the nucleus effectively react with assembly-competent tau in an extension reaction to form filaments (F) with extended β -sheet structure parallel to the axis of the fiber and perpendicular to the inducer surface (Kuret, Chirita et al. 2004). The elongation reaction will proceed spontaneously due to the energetically favorable property of this reaction.

1.5 Tables

Nomenclature		E2	E3	E10
3R isoforms	N0R3	-	-	-
	N1R3	+	-	-
	N2R3	+	+	-
4R isoforms	N0R4	-	-	+
	N1R4	+	-	+
	N2R4	+	+	+

.

Table 1.1 Nomenclature for six tau isoforms

This nomenclature clearly demonstrates the alternative splicing of the three exons: where “N*” indicates the N-terminal, the number “2” means there are exons 2 and 3 in the N-terminal of this isoform; number “1” means there is only exon 2 and “0” means there are neither of exon 2 nor 3 in the N-terminal. R3 or R4 indicates the exon 10-skipping three- repeat or the exon 10-containing four-repeat isoforms.

Types of Disease/Mutations	Isoform in Taupathology
Alzheimer's Disease FTDP-17	4R and 3R isoforms
Cortical Basal Degeneration Progressive Suprenulear Palsy Argyophilic Grain Disease	Only 4R isoforms
Pick's Disease	Only 3R isoforms

Table1.2 Tauopathies classified by the major associated tau isoforms

Tauopathies can be classified into three classes according to the types of isoform appeared in aggregation. The first class of tauopathies is caused by all six tau isoforms, like Alzheimer's disease. The second class is caused only by 4R isoforms. The vast majority of tauopathies fall into this class, like Cortical Basal Degeneration and Progressive Suprenulear Palsy. The third class includes a few rarely dementia that are entirely caused by 3R tau isoforms, like Pick's disease.

1.6 Figures

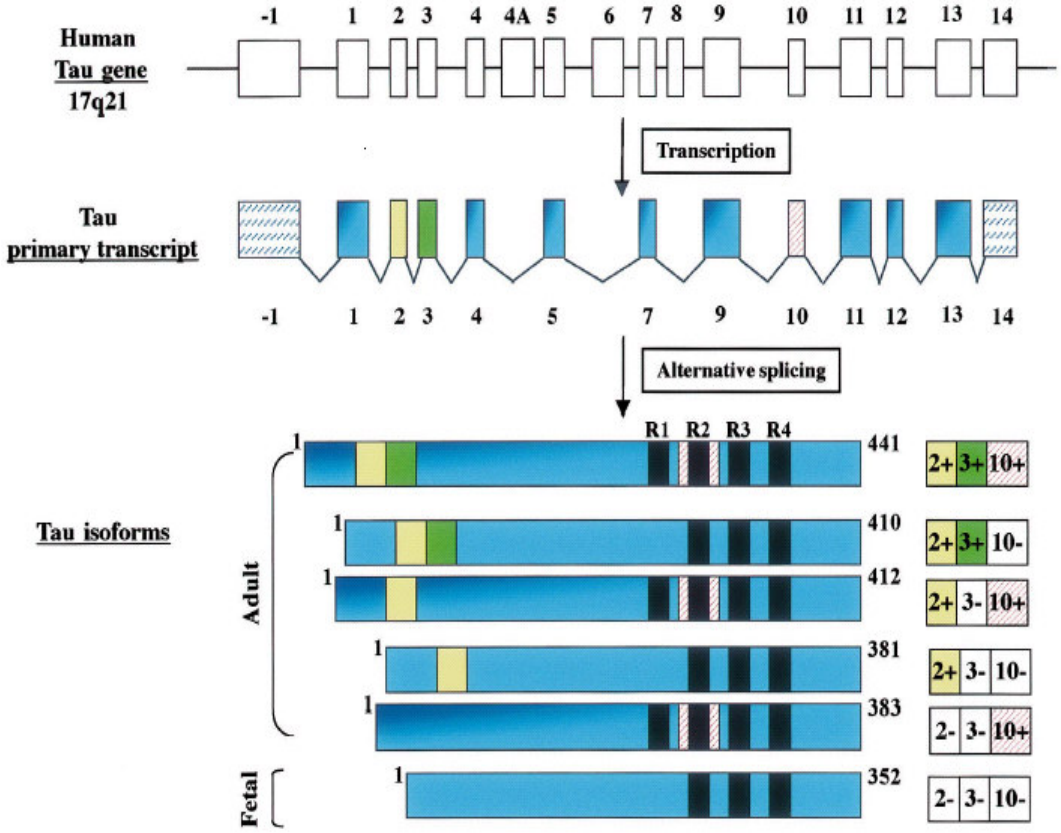

Brain Res Brain Res Rev 33(1): 95-130

Figure 1.1 Alternative splicing results in expression of six tau isoforms.

The human tau gene is located on the long arm of chromosome 17 and consists of 16 exons, of which 11 are expressed in the human brain. Exons 2, 3, 10 are alternatively spliced, leading to the presence of six different tau isoforms ranging from 352 to 441 amino acids. All the six isoforms have at least three microtubule binding domains. Exon 10 encodes an additionally fourth microtubule-binding domain. So the isoforms can be divided into two groups: 3R tau and 4R tau. The shortest isoform is predominantly expressed during early development, where isoforms with four repeats are expressed during adulthood.

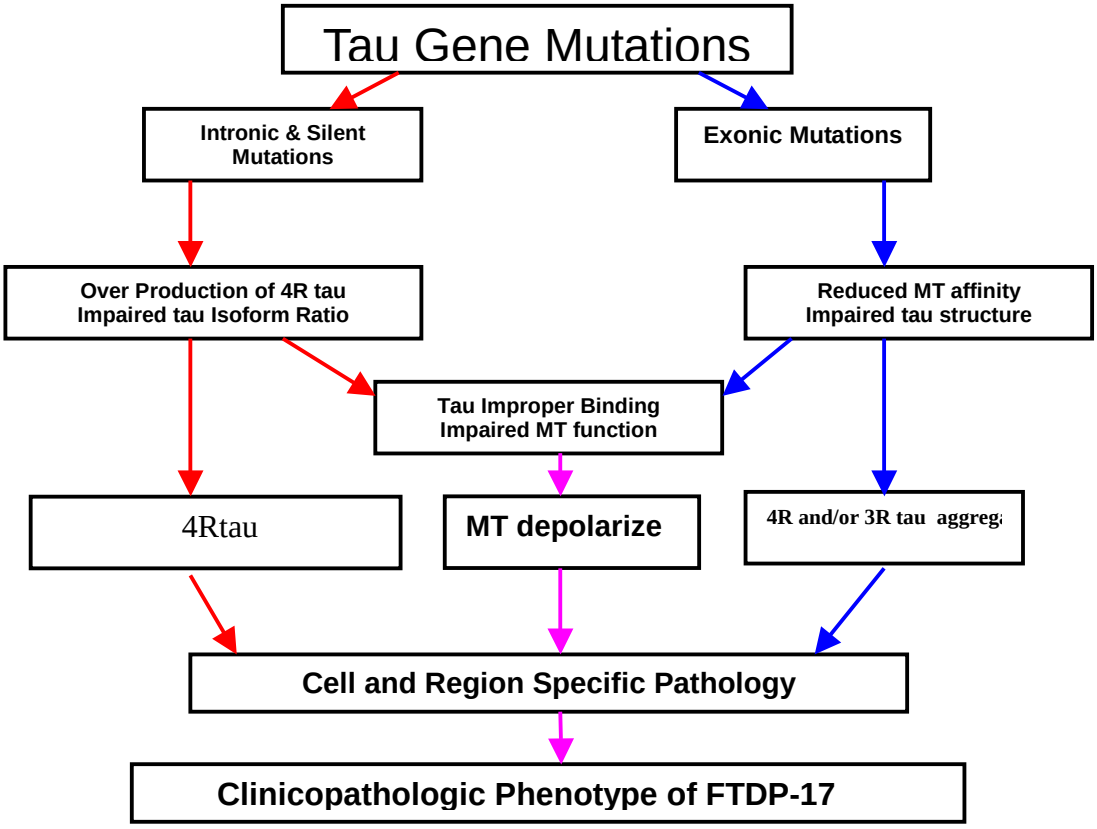

Figure 1.2 Possible mechanism explaining why tau gene mutations lead to disease formation.

For the red arrowed boxes, the intronic and silent mutations lead to overproduction of normal 4R tau isoforms. Increased 4R tau may result in an excess of tau over available 4R binding sites on microtubules. This abundance may lead to accumulation of unassociated 4R tau. Unbound tau is phosphorylated and precipitated into filaments in neuron. Over long period of time, large amounts of toxic tau filaments forms NFTs. It is well known that 4R tau possesses a greater ability to interact with microtubules than 3R tau, possibly 40-fold higher than that of 3R tau. The excess binding with 4R tau would result in an over-rigid and inflexible microtubule structure. Without proper binding with proper tau isoforms, microtubules will destabilize and depolarize. This will trigger a series of abnormalities in intracellular signaling and neuronal trafficking. Neurons are unable to maintain their morphology and function and eventually undergo neuronal death. For the blue arrowed boxes, the exonic tau mutations produce normal ratio of 4R/3R tau. However, they produce abnormal tau mutants and altered tau structure leads to much reduced affinity to bind to MTs. Without proper binding of tau, the function of MTs is impaired as mentioned above. Excess of unbond mutant tau is precipitated to form filaments. Under similar mechanism with those intronic mutations, neurons will undergo apoptosis and over time clinicopathologic phenotype will appear.

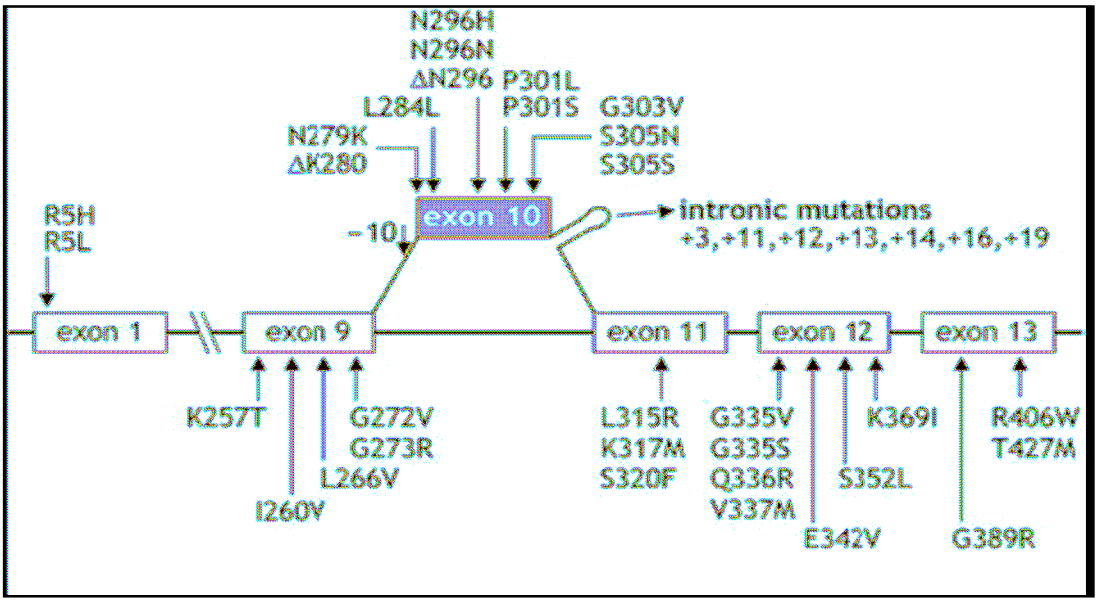

Class	Location	Exon 10 splice	4R/3R ratio	MT binding
I	**All intronic mutaions & Exonic silent mutations**	**Increase**	**Increase**	**No effect**
II	**Exonic missence & deletions mutations**	**No effect**	**No effect**	**Reduced**

(Hernandez and Avila 2007)

Figure 1.3 Cartoon showing FTDP-17 mutations on tau gene.

FTDP-17 mutations can be classified into two classes. One class consists of exonic missense and deletion mutations located within the coding sequence of tau gene and influences microtubule binding. Most of these exonic mutations are located in exon 9, 10, 11, and 12. They reduce the affinity of tau binding to microtubules and cause MT dysfunction. The second class consists of all intronic mutations and exonic silent mutations that affect the distribution of alternatively spliced tau isoforms. The intronic mutations are located on the intron following exon 10. This class of mutations has no effects on tau's binding to MTs and they produce six normal tau isoforms. However, they cause exon 10 to be excessively expressed, leading to significant increase in the amount of 4R tau.

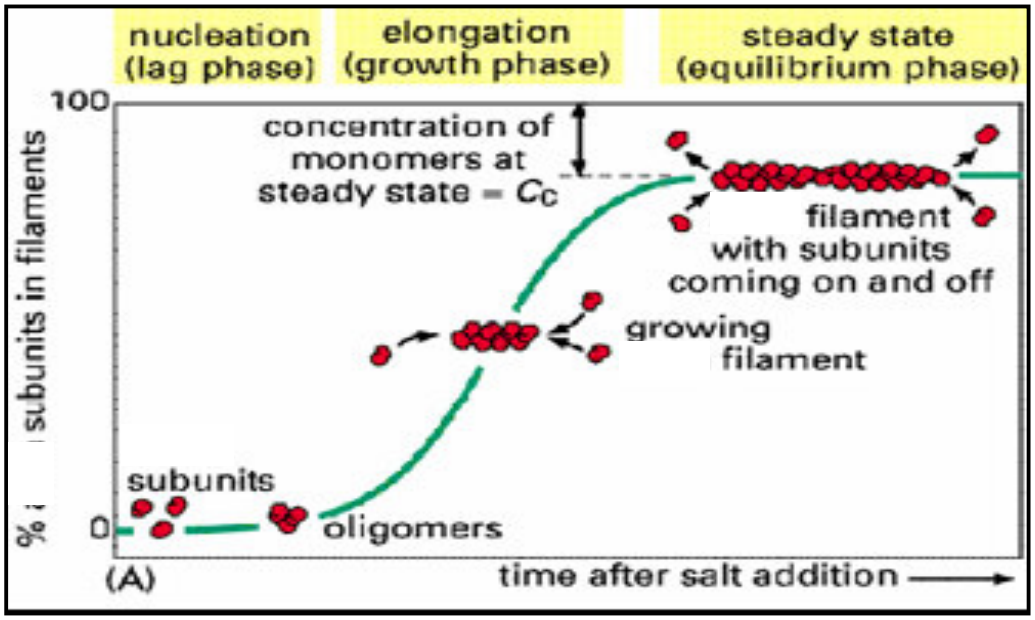

Figure 1.4 Tau fibrillization pathway *in vitro* follows the nucleation-elongation model.

The time course of fibrillization is composed of three phases: a lag time phase, a growth phase, and a steady state phase. During the lag time phase, no filament can be detected. The processes are characterized by a slow nucleation phase, in which the protein undergoes a series of unfavorable association steps to form an ordered oligomeric nucleus. A polymer is not observed until the monomer concentration exceeds a certain level known as the critical concentration (CC). In growth phase, the nucleus rapidly grows to form larger polymers. In steady state phase, the ordered aggregates and the monomer appear to be at equilibrium.

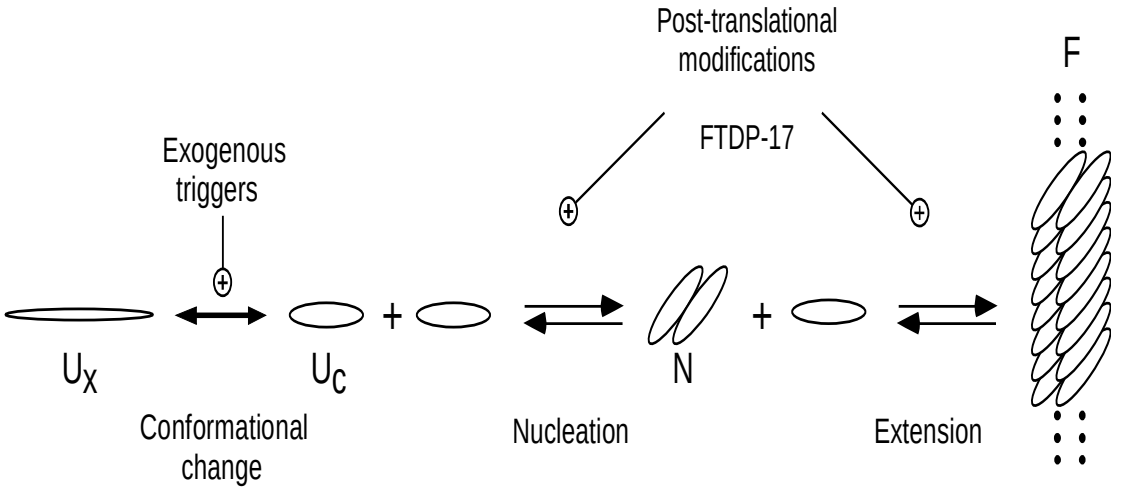

Figure 1.5 Hypothesized mechanism of tau fibrillization.

We hypothesize that the tau protein assembles via a modified nucleation dependent mechanism. The bulk of tau in solution exists as an assembly in competent monomer (Ux). Conformational change is achieved either spontaneously, in which case it may be stabilized by □ sheet binding dyes, or through the addition of exogenous inducers including anionic surfactants (arachidonic acid, alkyl sulfate detergents, anionic microspheres, etc) or polyanions (heparin, RNA, etc.). The conformational change results in the formation of the partially folded intermediate species (I) and potentially multiple other assembly competent species (Uc). Assembly competent species contain increased secondary structure and are capable of binding □-sheet selective molecules such as ThS. These intermediates then spontaneously aggregate until the critical nucleus size is reached. Once nucleation occurs the energetically favorable extension reaction can proceed. Posttranslational modifications, alternative splicing and mutations can potentially modify each of these steps. Data presented herein will address issues of reaction mechanism, nucleus cluster size and elementary rate constants for the nucleation and elongation reaction.

CHAPTER 2

2 CASEIN KINASE 1 ISOFORMS mRNA LEVELS ARE ELEVATED IN ALZHEIMER'S HIPPOCAMPUS

2.1 Introduction

The casein kinase I (CKI) family is a group of highly related, ubiquitously expressed serine/threonine kinases found in all eukaryotic organisms (Vielhaber and Virshup 2001). Six distinct subfamilies have been identified and recognized in human tissues and are designated as CK1-α,γ1, γ2, γ3, δ, ε (alpha, gamma 1, gamma2, gamma 3, delta, and epsilon) which are encoded by separate genes. These kinases share highly conserved N-terminal catalytic domains with striking similarity but can differ extensively in their C-terminal non-catalytic domains (Gross and Anderson 1998). Although both the function and regulation of these enzymes remained poorly uncharacterized in that they appeared to be constitutively active and were capable of phosphorylating an extensive number of proteins other than casein. Accumulated evidence has linked CK1 family to a diverse number of biological events. For example, CK1 can influence morphogenesis by acting in the Wnt singling pathway (McKay, Peters et al. 2001; McKay, Peters et al. 2001). Recent studies have confirmed roles for CKI in regulating circadian rhythm (Friedhoff, Schneider et al. 1998). Moreover, CK1 is

also involved in many other cellular processes including cell cycle progression (Gross, Simerly et al. 1997), membrane trafficking (Dubois, Kerai et al. 2001), and nuclear import (Hutton, Lendon et al. 1998).

Recently, CK1 has been indicated in the pathogenesis of Alzhemier's disease. One of the hallmark of AD is the development of intracellular deposits of hyperphosphorylated tau filaments and CK1 might potentially be a phosphotransferase involved in tau hyperphosphorylation (Kuret, Johnson et al. 1997). CK1 fulfils several criteria expected for a pathological tau protein kinase. First, CK1 isoforms are capable of phosphorylating tau *in vitro* at sites found in filamentous tau (Li, Yin et al. 2004). Second, CK1 homologs colocalize with NFTs in authentic AD tissue and also colocalize with granulovacoular bodies (GVBs) in AD hippocampus (King, Ghoshal et al. 2001). These bodies are one of the pathological hallmarks of AD. Not only associated with AD, The distribution of CK1 delta was studied by immunohistochemistry and correlated with the pathological hallmarks of many other neurodegenerative disorders including Down syndrome (DS), progressive supranuclear palsy (PSP), parkinsonism dementia complex of Guam (PDC), Pick's disease (PiD), pallido-ponto-nigral degeneration (PPND), Parkinson's disease (PD), dementia with Lewy bodies (DLB), amyotrophic lateral sclerosis (ALS) (Schwab C 1995). Lastly, the CK1 delta protein is overexpressed in AD hippocampus relative to age-matched controls (King, Ghoshal et al. 2001).

Although so many observations have led to the hypothesis that CK1 enzymes contribute to the hyperohosphorylation of tau in AD, it is still not confirmed that CK1 isoforms phosphorylate tau in real disease and lead to neurodegeneration. In order to

further test the hypothesis, it is important to find out whether there are any changes of the mRNA levels of each CK1 isoform in AD brain compared to normal brain. In this study, I measured the mRNA expression levels of the six CK1 isoforms in human post-mortem hippocampus. I used a real-time RT-PCR technique to quatitatively compare the relative mRNA expression levels of CK1 isoforms between Alzheimer's disease brains and age-matched normal brains.

2.2 Materials and method

2.2.1 Post-mortem brains sample collection

A total of 12 post-mortem brain specimens of AD patients and age-matched controls were obtained from the Rochester university medical center. Six specimens were from patients diagnosed with AD, and six were from age-matched control subjects. **Table 2.1** shows the details of the age, gender, and post-mortem delay hours for each case. All cases were above the age of sixty-five, the post-mortem dalay hours were all less than twenty-fours. All samples dissected were stored frozen at –80 ºC.

2.2.2 Oligonucleotide primers for RT-PCR

The primers for real-time RT-PCR (**Table 2.2**) were designed using PrimerSelect 4.00 software (RNASTAR Inc). Every pair of primers was designed to flank a region that contains at least one intron to avoid amplification of genomic DNA. Criteria taken into consideration during probe design were (i) a probe length of between 20 and 30 nucleotides, (ii) a calculated probe-annealing temperature 5–10°C higher than the

calculated product-annealing temperature, (iii) a lack of predicted dimer formation with the corresponding primers, (iv) a lack of self-annealing potential, (v) product length between 100bp to 500bp. GAPDH (glyceraldehyde-3-phosphate dehydrogenase) were used as internal standard.

2.2.3 Total RNA extraction

50-100 mg dissected brain tissue from each patient was homogenized by sonicator (Fisher Scientific, CA). The CA1 region of the hippocampus of the brain tissue was dissected on dry ice quickly and the total RNA was extracted immediately after dissection. Total RNA was isolated using a TRIzol reagent (Invitrogen, CA) according to the manufacturer´s recommendations (Hartig, Klein et al. 2000). The concentration of total RNA samples was ascertained by measuring the optical density at 260 nm. The quality of RNA was confirmed by the detection of 18S and 28S bands after agarose-formaldehyde gel electrophoresis. To remove residual genomic DNA contamination, the RNA samples were incubated with RNAse-free DNAse I (Invitrogen, CA) at RT for 15 min, and then each reaction was terminated by adding 1 ul 25mM EDTA and heat at 65 °C for 10 min (Dunckley, Beach et al. 2006). The mixture was either used directly for reverse transcription or kept frozen at –20 ºC for future use.

2.2.4 Real-time semi-quantitative one-step RT-PCR

A single-tube, single-step method was used for RT-PCR according to manufactures recommendations (QIAGEN QuantiTect SYBR Green RT-PCR kit) (Beuve, Sempe et al. 2007). Real-time quantitative PCR amplification reactions were carried out in a Biorad iCycler detection system (Bio-rad) in a 25 ml volume. The reaction mixture consisted of 12.5 ul 2× QuantiTect SYBR Green RT-PCR Master Mix (containing HotStarTaq DNA Polymerase; RT-PCR buffer; SYBR-Green 1 as reporter dye; 5 mM $MgCl_2$; dNTP Mix including dUTP; ROX (passive reference dye)), 5 ul primer pair with final concentration of 0.5uM, 0.25ul QuantiTect RT mix. 12.5 nanogram of total RNA template was added to each reaction. The reaction was subjected to a pre-cycle condition consisting of 30 min at 50 °C (for reverse transcription), 15 min at 95 °C followed by 40 cycles of amplification. Each cycle consisted of 94 °C for 15 s, 55 °C for 15 s and 72 °C for 30 s (Escutenaire, Mohamed et al. 2007; Santhosh, Parida et al. 2007). All reactions were carried out in triplet with template negative controls. The fluorescent spectra were recorded during the elongation phase of each PCR cycle. After RT-PCR, ten percent of the amplified product was loaded in an agarose gel (2%) containing 0.5 ug/ml ethidium bromide for electrophoresis. RT- PCR products were mixed with a sample loading buffer and visualized by examination under UV light after separation on agarose gel.

2.2.5 Threshold cycle (C_T) values

RT-PCR reactions were monitered by computer connected to the iCycer and an amplification plot of the PCR products in every PCR cycle is generated for each reaction. Threshold cycle (C_T) value was the cycle number at which the SYBR green fluorescence generated within a reaction crosses the threshold within the linear phase of the amplification profile (Lo, Yip et al. 2007). The C_T-value is an important quantitative parameter in real-time PCR analysis. To reach to the same level of fluorescent threshold, reactions with larger amount of starting mRNA present smaller number of threshold cycle number. So, by comparing the C_T value, we can compare the relative mRNA levels in brain tissues. The amplification plots and C_T-values were exported from the exponential phase of PCR directly into a Microsoft Excel worksheet for further analysis (Graham, Taylor et al. 2006).

2.2.6 Melting curves and standard curves

After running real time RT-PCR, to distinguish specific amplicons from non-specific amplifications, a melting curve could be extracted form the computer software for each CK1 isform and GAPDH. Sharp, single pick in the melting curve ensures the pure PCR product. The melting curve was constructed incubating the amplification products from 60 to 90°C with an increase of 0.28C/sec. The melting temperature (Tm) values of the specific amplicons were in the range of 75–86°C (**Figure 2.1**), whereas the

Tm primer–dimer values were found to be below 70-74°C. To ensure the 100% PCR efficiency for each reaction/isoform, the total RNA samples were diluted serially and each dilution was used in the real-time RT-PCR for the construction of a standard curve for all CK1 isoforms and GAPDH. Plotting C_T against log dilution of starting total RNA (14ng, 24.5ng, 43ng, 75ng, 141ng) produced a linear relationship (r^2=0.988) for all CK1 isoforms and GAPDH, demonstrating the quantitative nature of the real time RT-PCR method and the PCR efficiency is close to 100% (Dos Santos, Poloni et al. 2008).

2.2.7 Relative quantification and statistics analysis

To compare GAPDH and CK1 isoforms, a comparative C_T method was used according to Aarskog and Vedeler (Aarskog and Vedeler 2000), and Sieber et al (Siebert, Neumann et al. 2002). Briefly, this comparative C_T method involved averaging triplecate samples taken as the C_T-values for CK1 isoforms and GAPDH. The ΔC_T-value was obtained by subtracting the average C_T-value of GAPDH from the average C_T-value of CK1 isoforms. The present study used the average ΔC_T of six control cases as the calibrator. The fold change was calculated according to the formula $2^{-(\Delta\Delta C_T)}$, where $\Delta\Delta C_T$ was the difference between ΔC_T value (AD group) and the ΔC_T calibrator value (control group). Student *t* test is used to determine the *P* value of each CK1 isoform. $P<0.05$ is considered of statistical significance.

2.3 Results

2.3.1 All CK1 iforms exist in AD and control brains

Using real time RT-PCR, the existence of the six CK 1 isoforms (alpha, delta, gamma1, gamma2, gamma3, and epsilon) were all identified in the CA1 region of the hippocampus of all cases. The RT-PCR products ranging from 125 bp to 270 bp for each CK1 isoforms and GAPDH were sequenced and were identical to the published CK1 sequences. Our results demonstrate that the six CK1 isoforms are consistently expressed in both AD and normal brain (**Table 2.3**).

2.3.2 CK1 isoforms are unevenly expressed in human brain

However, the mRNA expression levels of the six CK1 isoforms were not the same. The average C_T numbers (**Table 2.3**) for CK1-dleta was the lowest in both AD (21.08) and control groups (25.48), indicating the highest mRNA expression level among all these six isoforms. CK1-gamma 1 had the highest C_T numbers in both AD (27.83) and control groups (30.66), indicating the lowest mRNA express level among isoforms. The differences between the threshold cycle numbers among CK1 isoforms in AD as well as control groups demonstrate the differential mRNA expression pattern among CK1 isoforms. The heterogeneous expression pattern indicates the heterogeneous activity of each CK1 isoform in CA1 region of hippocampus where the highest staining for NFTs and Plaques is observed.

2.3.3 CK1 delta and gamma 2 mRNA levels are elevated in AD Brain

CK1 delta (P=0.046) mRNA has the most significant AD/control ratio of 13-fold up-regulated in AD hippocampus comparing to age-matched non-AD cases. CK1 gamma 2 (p=0.004) mRNA has about 4-fold increase in AD brains. No statistical difference between AD and control groups were found for CK1 alpha, gamma 1, gamma 3 and epsilon (P>0.05) (**Table 2.4**).

2.4 Discussion

Phosphorylation of serine, threonine and tyrosine residues by cellular protein kinases plays an important role in the regulation of various cellular processes. In recent years our knowledge of the regulation and function of serine/threonine specific casein kinase 1 family members has rapidly increased. Mammalian CK1 isoforms are involved in diverse cellular processes including membrane trafficking, circadian rhythm, cell cycle progression, chromosome segregation, apoptosis and cellular differentiation. Deregulation and/or the incidence of mutations in the coding sequence of CK1 isoforms have been linked to various diseases including neurodegenerative disorders such as Alzheimer's and Parkinson's disease (Knippschild, Wolff et al. 2005).

Quantification of CK1 isoform mRNA using real-time RT-PCR showed increased CK1 isoform delta and gamma 2 mRNA levels in the CA1 region of AD brain which carries the heaviest pathological burden. Our data, in parallel, is in agreement with

several previous observations. First, western blot analysis has shown an upregulated CK1 delta protein level in AD (King, Ghoshal et al. 2001). Here we have shown that the elevated CK1 delta protein levels accompanying formation of AD pathology can be accounted by increases in total CK1 delta mRNA. Second, CK1 family is copurified with authentic PHFs (Kuret, Johnson et al. 1997). Third, many studies have shown that CK1 can phosphorylate tau *in vitro* (Wang, Wang et al. 2002) (Li, Yin et al. 2004) (Yin and Kuret 2006). Many of the phosphorylation sites are identical to thoes sites found in AD patients. A combination of casein kinase 1 delta and glycogen synthase kinase-3beta activities could account for over three-quarters of the serine/threonine phosphorylation sites identified in PHF-tau, indicating that CK1 delta may have a role, together with glycogen synthase kinase-3beta, in the pathogenesis of Alzheimer disease (Hanger, Byers et al. 2007). Fourth, The high level of CK1 expression in CA1 region is supported by immunohistochemistry result which showed extensive colocalization with neuritic tangles and plaques (Kannanayakal, Tao et al. 2006), (Kannanayakal, Mendell et al. 2008). Lastly, the protein p 42 (IP4) (also called centaurin alpha) is a brain-specific InsP4/PtdInsP3 (PIP3)-binding protein. It was reported to possess a binding domain for casein kinase 1 and its immunostaining is also increased in AD cases comparing to control cases. Thus, the up-regulated p42 (IP4) in AD neurons may serve as a docking protein to recruit up-regulated CKI to the plasma membrane (Reiser and Bernstein 2002). In summary, our RT- PCR data further support that CK1 is highly associated with AD, especially the isoform delta and gamma 2, indicating that CK1 is a highly involved

candidate kinase for the pathological hyperphosphorylation of tau protein and its assembly into neurofibrillary lesions.

The two classical pathological hallmarks of Alzheimer's disease are deposits of aggregated beta-amyloid peptide and neurofibrillary tangles composed of hyperphosphorylated tau protein. CK1 is not only involved in tau hyperphosphorylation, but also involved in the formation of neurotoxic amyploid plaques by the phosphorylation of the amyloid precursor protein (Walter, Schindzielorz et al. 2000). One recent study found that overexpression of constitutively active CK1 leads to an increase in A-beta peptide production. Conversely, inhibit CK1 significantly reduced endogenous Abeta peptide production (Flajolet, He et al. 2007). These findings indicate that increased CK1 mRNA levels contribute to the pathogenesis of AD not only through the tau pathway, but also beta-amyloid pathway.

Our RT-PCR results found that CK1-γ2, and δ are statistically increased to 4-fold and 13-fold. However, there are no significant difference in for CK1-α, γ1, γ3, and ε. The result indicates that different CK1 isoforms are differencially involved in biological or pathological processes (Hutton, Lendon et al. 1998). CK1-delta and gamma2 may play a bigger role in AD pathological process in the hippocampus than the other CK1 isoforms (Kannanayakal, Tao et al. 2006). Indeed, CK1-epsilon has been highly active in regulating the circadian rythems (Meng, Logunova et al. 2008). CK1-alpha is in great association with mitotic spindles in cell cycle progression (Dubois, Howell et al. 2002).

CK1 gamma isoforms have been poorly characterized as to their physiological or pathological roles.

Yasojima et al. showed in 2000 that CK1 delta mRNA level is increased about 24-fold in AD hippocampus relative to controls (Yasojima, McGeer et al. 1999). Although the actual numbers are different, they do reveal a trend of significant upregulation of Ck1 delta mRNA in AD brains. The difference in results between our studies and theirs may due to different sample size, gender, age, time of sample preparation (early versus late postmortem delay) (Preece and Cairns 2003), different disease stages (early versus late stage of AD), internal control used to normalization, and/or differences in methodologies used for quantification of mRNA signals (microarray versus real-time RT-PCR or conventional RT-PCR). However, the two studies agree that the mRNA levels of CK1 delta were increased in AD cases comparing to control cases. Our study is the first RT-PCR study to investigate all CK1 isoforms side by side.

GAPDH is considered as a house keeping gene and is used widely as a internal control in many studies (Harrison-Bernard, El-Dahr et al. 1999; Freund, Pons et al. 2002; Wang, Wang et al. 2002). Our results showed that GAPDH mRNA expression is stable in AD and normal brain, and can be used as the internal control. Our founding is consistence with the Gutala's and Meldgaard's results respectivly. They both specifically used RT-PCR to study GAPDH in AD brain and they claimed that GAPDH could be validly used as a endogenous reference gene in the study of AD brains (Gutala and Reddy 2004) (Meldgaard, Fenger et al. 2006).

Although, significant evidence has indicate that CK1 is highly related to AD, CK1 is not the only kinase play this role. Many other kinases are also responsible for the pathogenic hyperphosphorylation of tau. Many other candidate kinases have been investigated including glycogen synthase kinase (GSK-3), cyclin-dependant kinase-5 (Cdk-5), MAPK family members (extracellular signal-regulated kinases 1 and 2 [Erk-1 and 2], MEK [MAP kinase kinase], c-Jun NH(2)-terminal kinases (JNKs) and p38), calcium calmodulin-dependant kinase II (CaMK-II), microtubule affinity regulating kinase (MARK), protein kinase A (PKA/cAMP-dependant protein kinase) and others (Churcher 2006). Itentify and inhibit these kinases responsible for pathogenic hyperphosphorylation will provide new target for the treatment of AD.

2.5 Summary

Tau is hyperphosphorylated as a result of an imbalance of the kinase and phosphatase activities that normally tightly regulate its phosphorylation. In addition to this pathogenic hyperphosphorylation, tau dissociates from microtubules and self-aggregates to form insoluble oligomers which progress to the macroscopic tangles evident in post mortem Alzheimer's disease tissue. Our RT-PCR results have demonstrated that CK1 isoforms mRNA is upregulated in AD hippocampus versus control cases, especially Ck1 delta which was elevated to 13-fold and gamma 2 which was elevated to 4-fold. The rest of CK1 kinases (alpha, gamma1, gamma2 and epsilon) do not shown to have a difference between AD and control groups. The elevated mRNA

expression level in AD suggests that CK1 isoform delta and gamma 2 are highly involved in AD pathogenesis.

2.6 Supplementary data analysis

If I normalize each of the C_T-value for CK1 isoforms to each of the corresponding C_T-value of GAPDH case by case, instead of using the average C_T-value for CK1 isoforms and the average C_T-value for GAPDH, there will be a greater difference among the cases in the ΔC_T values (AD group) as well as the ΔC_T calibrator values (control group. Thus, the *P* value of each CK1 isoform will be greater than 0.1 and there will be of no statistical significance between my six AD cases and six control cases for all of the CK1 isoforms. To overcome this limitation, larger sample size is needed to help to reach a more accurate conclusion.

2.7 Tables

Cases	Age (years)	Gender	Postmortem delay (hour)
Control			
C1 (99A-114)	**87**	**M**	**15**
C2 (99A-124)	**66**	**M**	**5**
C3 (99A-189)	**91**	**F**	**6**
C4 (99A-204)	**73**	**F**	**8**
C5 (99A-287)	**89**	**M**	**10**
C6 (99A-290)	**77**	**F**	**21**
AD			
A1 (98A-201)	**86**	**M**	**17**
A2 (98A-236)	**77**	**F**	**16**
A1 (98A-286)	**84**	**F**	**9**
A1 (99A-016)	**74**	**M**	**5**
A1 (99A-021)	**87**	**F**	**9**
A1 (98A-230)	**80**	**F**	**18**

Table 2.1 Age, gender and postmortem delay hours for six AD cases and six control cases.

Gene names	Forward primer Reverse Primer	Size of amplicon (bp)
CK1-α	5'-GGTGGTATGGTCAGGAAAAAGA-3' 5'-CTGTTGTCTCTGTACTTTTTGG-3'	274
CK1-γ1	5'-TTGGCAGTGCAGGTGAAGGTC-3' 5'-TCGGTCACAGAGGTCAAACAA-3'	122
CK1-γ2	5'-GCTATGTGCGGCGCCTGGACTTC-3' 5'-CGATGGGGGTCGGCAGGGGCTTC-3'	141
CK1-γ3	5'-GCAAGGCTTAAAGGCTGACACAT-3' 5'-ACGAAGCTATGTTGCCATTTCTG-3'	128
CK1-δ	5'-CTCACACACGGCTAACACCTCC-3' 5'-TGTGAGGTGGACATGCGAGAGG-3'	129
CK1-ε	5'-CGTCAGCTCTTCCGCAACCTCTTC-3' 5'-ATCCTCTCCTCGCGTTCGTGTTC-3'	143
GAPDH	5'-GGGGAGCCAAAAGGGTCATCATCT-3' 5'-AGGGGTGCTAAGCAGTTGGTGGTG-3'	150

Table 2.2 Primers and size of amplicons for each CK1 isoform and GAPDH.

Cases	CK1-α	CK1-γ1	*CK1-γ2	CK1-γ3	*CK1-δ	CK1-ε	GAPDH
A1	24.75	30.25	24.77	29.25	22.80	28.75	22.00
A2	27.77	30.45	24.80	30.30	23.90	28.20	22.50
A3	31.47	34.70	21.60	29.95	24.10	29.50	24.60
A4	22.75	25.71	23.30	23.80	21.00	24.73	21.12
A5	21.05	22.20	21.71	21.85	15.57	22.80	19.15
A6	21.30	23.70	24.80	25.15	19.10	22.50	18.40
C1	23.65	29.05	25.50	27.10	21.50	27.05	19.80
C2	32.40	31.57	26.30	30.15	28.75	33.25	23.95
C3	27.17	32.75	26.90	28.65	21.00	27.50	22.15
C4	37.05	30.20	26.50	29.85	29.57	33.03	28.15
C5	23.90	29.40	24.87	26.60	26.40	23.90	22.85
C6	26.57	31.00	27.20	28.65	25.63	29.27	15.00

*** $p<0.05$**

Table 2.3 Threshold cycle numbers for CK1 isoforms and GAPDH.

Gene name	Average C_T for AD cases	Average C_T for control cases	P-value	Fold-up
CK1-alpha	24.85	28.44	0.217	N/A
*CK1-delta	21.08	25.48	0.046	**13**
CK1-gamma1	27.83	30.66	0.193	N/A
*CK1-gamma2	23.5	26.21	0.004	**4**
CK1-gamma3	26.72	28.5	0.284	N/A
CK1-epsilon	21.08	25.48	0.155	N/A
GAPDH	21.29	21.98		

***** P<0.05

Table 2.4 Average threshold cycle numbers (C_T), P-value, and fold increase for CK1 isoforms.

2.8 Figures

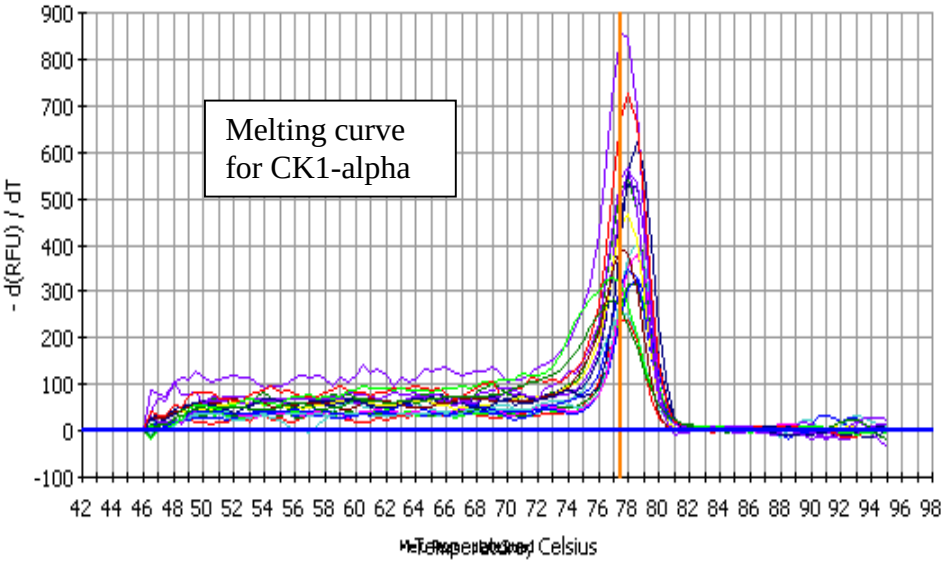

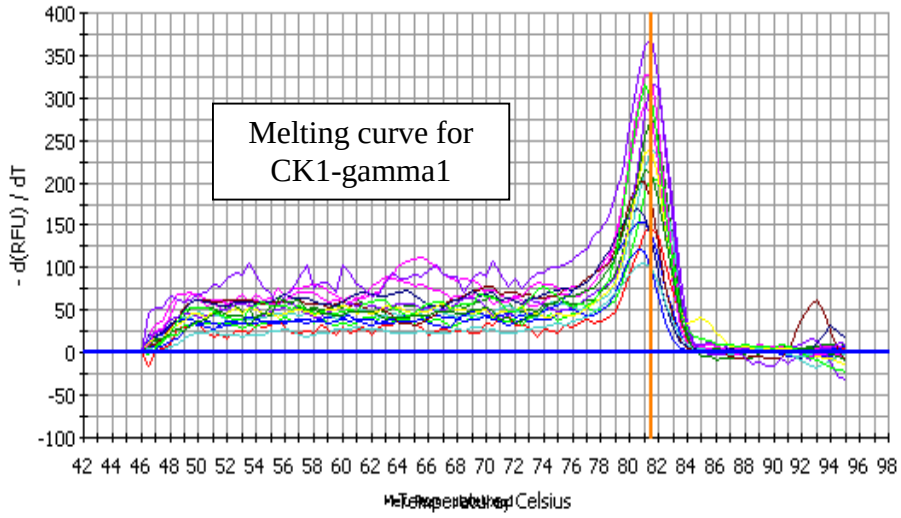

Figure 2.1 Meltting curves for CK1 isoforms (continued).

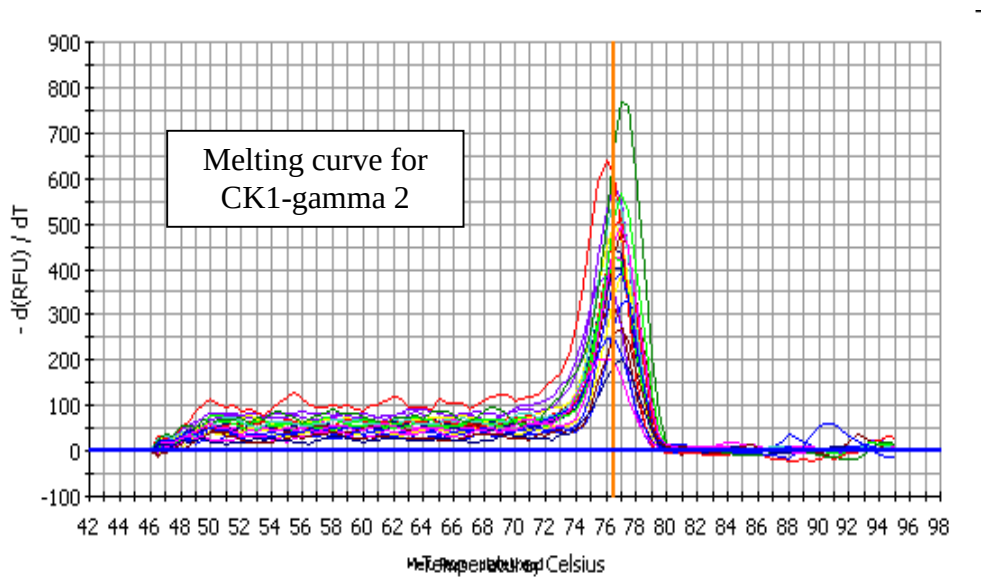

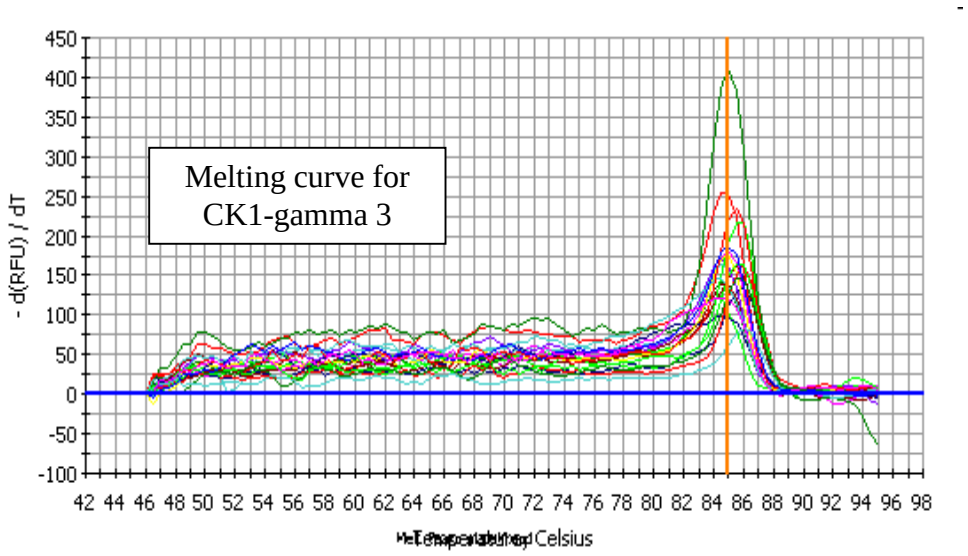

Figure 2.1 Meltting curves for CK1 isoforms (continued).

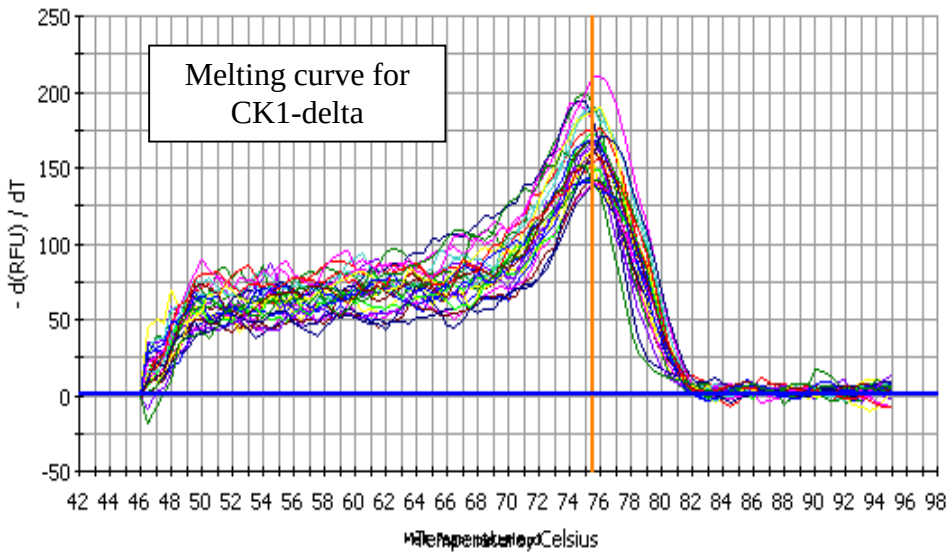

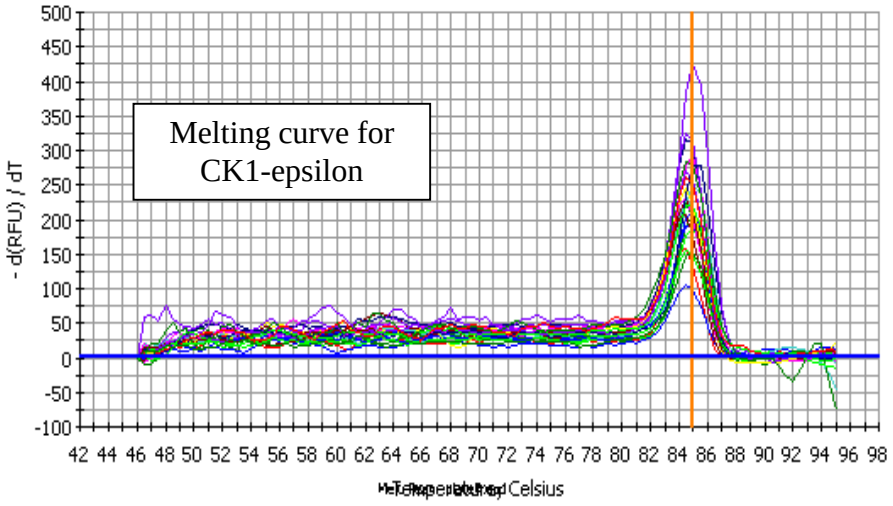

Figure 2.1 Meltting curves for CK1 isoforms (continued).

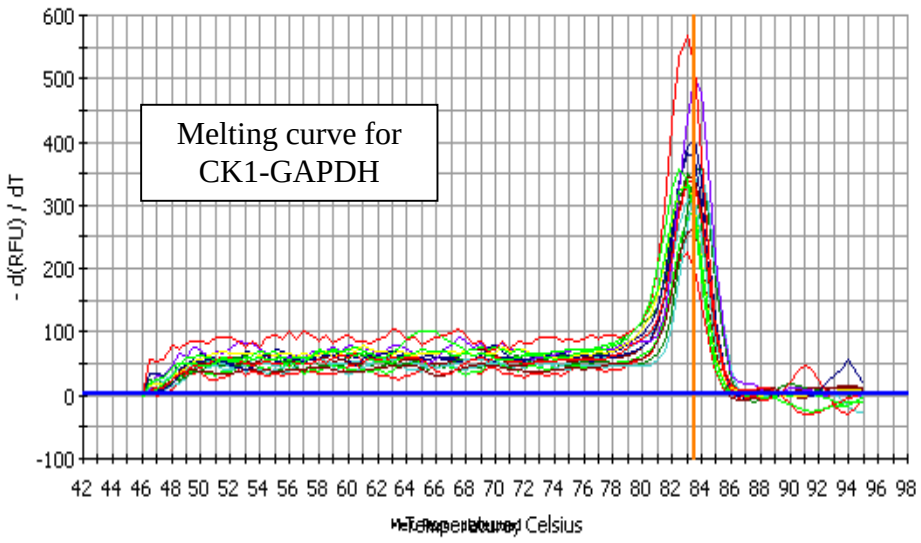

Figure 2.1 Melting curves for six casein kinase isoforms.

CHAPTER 3

3 ISOFORM STUCUTRE INFLUENCE TAU AGGREGATION

3.1 Introduction

Tau is a cytosolic protein widely exists in a variety of neurons in the central nervous system (Avila* 2007). The main physiological function of tau is to promote the assembly and stabilization of microtubules, which is essential for normal axonal transport of vesicles(Feinstein and Wilson 2005). The human tau gene is located on the long arm of chromosome 17 and consists of 16 exons, of which 11 are expressed in brain (Wszolek, Tsuboi et al. 2006). In the central nervous system, exons 2, 3, 10 are alternatively spliced, leading to the presence of six major different tau isoforms ranging from 353 amino acids in the shortest fetal isoform to 441 amino acids in the longest isoform (Avila 2004). All isoforms share a conserved C-terminal domain containing microtubule-binding repeats and a N-terminal projection domain of varying size (Abeliovich, Schmitz et al. 2000; Dehmelt and Halpain 2005). All of the six isoforms have at least three microtubule binding domains (MBD) encoded by exons 9, 11 and 12. Exon 10 encodes the second repeat on the MBD (2R). Based on the presence or absence of 2R, the six isoforms can be divided into two groups: three-repeat (3R) tau isoforms (N0R3, N1R3, N2R3) and four-repeat (4R) tau isoforms (N0R4, N1R4, N2R4) (Avila* 2007). Tau

isoforms are differentially expressed during early development (Takuma, Arawaka et al. 2003). The shortest isoform N0R3 is predominantly expressed in the fetal brain and during the first days of postnatal development. While all six isoforms are expressed during adulthood (Kosik, Orecchio et al. 1989).

Filamentous tau deposits in neurons or glia cells constitute a defining characteristic of several neurodegenerative diseases collectively called tauopathies. This family includes Alzheimer's disease (AD), Frontotemporal dementia and parkinsonism linked to chromosome 17 (FTDP-17), corticobasal degeneration (CBD), progressive supranuclear palsy (PSP) and Pick's disease. In 1998, several groups identified that intronic mutations in the tau gene lead to FTDP-17 with insoluble aggregates similar to neurofibrillary tangles (NFTs). There are no amyloid plaques in FTDP-17 mutations and the disease phenotype is dominant (Spillantini, Van Swieten et al. 2000). The intronic mutations of FTDP-17 lead to an overexpression the 4R tau isoform. This provides the evidence that abnormalities in gene expression are sufficient to cause filamentous aggregation of hyperphosphorylated tau and neurodegeneration.

Over 100 families with at least 39 different mutations in the tau gene have been identified in FTDP-17 cases worldwide(Gasparini L 2007). Intronic mutations are located at positions +3, +12, +13, +14, +16 and +19 of the intron following exon 10, with the first nucleotide of the splice-donor site taken as +1 (Hernandez and Avila 2007). All the intronic and some of the missense mutations in exon 10 were shown to cause exon 10 to be excessively expressed, leading to an overexpression of 4R tau as compared to 3R tau (Ko, DeTure et al. 2005). Normal adult human brain expresses roughly equal

amounts of 4R and 3R tau (Hutton, Lendon et al. 1998). However, the FTDP-17 mutations generally lead to a significant increase in the amount of 4R tau and raise the normal 4R/3R ratio from 1 to 2-3 (D'Souza, Poorkaj et al. 1999) (D'Souza and Schellenberg 2005). These findings show that changes in isoform ratio In fact, increased 4R isoforms have been identified in most other types of tauopathies. 4R tau mRNA was found to be elevated in AD(Yasojima, McGeer et al. 1999), PSP(Takanashi, Mori et al. 2002), CBD(Takanashi, Mori et al. 2002), and frontotemporal lobar degeneration(FTLD)(Ingelsson, Ramasamy et al. 2007). Therefore, altered ratios of tau isoforms clearly influence the activity and effects of tau and lead directly to filament formation and neurodegeneration.

However, the mechanisms by which altered 4R/3R ratio leads to tau aggregation are not clear. An investigation into the different aggregation properties of tau isoforms is urgently important. Tau fibrillization pathway *in vitro* follows the nucleation-elongation model. The kinetics of nucleation-dependent polymerization is characterized by two important factors: critical concentration and elongation lag time. Obtaining and comparing the kinetic of the 4R vs. 3R tau isoforms is of significant importance in the understanding the mechanism underlying pathological tau fibrillization.

3.2 Methods

3.2.1 Materials

Six recombinant poly-his tagged tau isoforms were prepared as described previously. Thiazine red was obtained from TCI America (Portland, OR) and stock

solutions were prepared in distilled water. Glutaraldehyde, uranyl acetate, and formvar-coated 300 mesh copper grids were purchased from Electron Microscopy Sciences (Ft.Washington, PA).

3.2.2 Tau isoform purification

To study the *in vitro* fibrillization, the first step is to obtain pure protein. E. coli MM 294 cells were transformed with isoform-specific pT7C vector(King, Gamblin et al. 2000). For purification of recombinant histidine-tagged tau protein, cells were lysed in 500 mM NaCl, 5 mM imidazole, and 10 mM Tris (pH 8.0) using a French Pressure Cell Press (American Instrument Co.). Lysates were centrifuged at 100,000 *g*. This is followed by purification by affinity chromatography using nickel columns, followed by further purification on gel filtration (Carmel, Leichus et al. 1994; King, Gamblin et al. 2000). Tau isoforms were fused to an N-terminal, 20 residues peptide containing histidines. Although tau resulting from this purification procedure is histidine-tagged, it has been shown that the tag does not interfere with either filament morphology or tau filament formation (King, Gamblin et al. 2000). The quality of all preparations was assessed by SDS-PAGE (**Figure 3.1**), and final protein concentrations were calibrated on the basis of optical density (Carmel, Mager et al. 1996). Tau protein concentrations were determined by absorbance at 280 nm (Carmel, Mager et al. 1996). Proteins are all diluted in to the same concentrations (2.5 mg/ml) and stored in -20 ºC.

3.2.3 Fibrillization assays

All tau isoforms were incubated without agitation in assembly buffer containing 10mM HEPES (pH 7.4), 100mM NaCl, and 5 mM Dithiothreitol (DTT) for up to 24 hours at 37^{o}C. Thiazine red (100 μM) was added to the reaction mixture to induce polymerization. In preparation for electron microscopy, Aliquots (50 μL) of aggregation and reactions are removed, fixed with glutaraldehyde (2%), and adsorbed (1 min) onto 300 mesh formvar/carbon-coated copper grids (Electron Microscopy Sciences; Ft. Washington, PA). The resultant grids are washed with water, stained (1 min) with 2% uranyl acetate (Electron Microscopy Sciences), washed again with water, blotted dry, and viewed in a Phillips CM 12 microscope operated at 65 kV. Four to five random images from each experimental condition are captured on film at 22,000x magnification, digitized, calibrated, and imported into Optimas 6.5.1 for quantification of total filament length as described previously (King, Gamblin et al. 2000). Individual filaments were counted manually. All filaments 10 nm or longer were used for analysis and results were calculated as total filament length per field ± the standard deviation.

3.2.4 Determination of critical concentration

Varying concentrations of each tau isoform were added to reaction mixtures containing buffer, 5 mm DTT, and 100 μM thiazine red from serially diluted stocks. Samples were incubated at 37^{o}C for 24 hours, allowing the reactions to come to

equilibrium. Aliquots were then prepared for electron microscopy and images collected as described above. Total filament length per field ± the standard deviation was plotted as a function of tau concentration. Data was fit to a linear function and the abscissa intercept, or critical concentration, was determined for each isoform.

3.2.5 Determinations of k_{off} and k_{on}

A reaction mixture, including 100 μM thiazine red was prepared as described above for each tau isoform and incubated at 37^{o}C for 24 hours. After incubation the mixtures were diluted ten-fold such that the concentration of tau in each sample was below the critical concentration. One hundred μL aliquots were withdrawn each hour between one and five hours post-dilution. Samples were fixed, mounted, and stained as described and images were collected. Total filament length and total filament number were determined for each isoform and time point. Data from the dissociation time courses was plotted as natural log of total filament length against time in seconds (Kristofferson, Karr et al. 1980; Necula, Chirita et al. 2005). The data was fit to a linear function and the slope of each resultant line was determined. This value represents the apparent rate constant, k_{app}. This figure can then be used to calculate the actual dissociation constant k_{off} using this Equation (1). Where L_0 is equal to the total filament length at time 0, and [ends] represents the total number of filaments. Data from the STEM analysis provides that the value for number of monomers per nanometer is 3.9.

$$k_{off} = \frac{L_0}{3.9} \times \frac{k_{app}}{[ends]} \quad (1)$$

The resulting k_{off} was then used to calculate the forward elongation constant k_{on} using equation (2). Where K_{crit} is the critical protein concentration. These calculated results were then incorporated into the mathematical model.

$$k_{on} = \frac{k_{off}}{K_{crit}} \quad (2)$$

3.2.6 Time courses

Fibrillization time courses were carried out at a constant supersaturation, 0.3 μM above the critical concentration, for each isoform. Reactions were incubated for 24 hours with aliquots withdrawn at specific time points (15, 30, 45, 60, 90, 120, 180, 240, 300, 420 min and 24h), fixed with 2% glutaraldehyde, and mounted on grids for electron microscopy. Random images were collected from each time point and isoform with total filament length determined as described above. Time courses were fit to Gompertz functions and lag times were determined.

3.2.7 Isoform dominance

Recombinant human N2R4 and N0R3, the longest and shortest isoforms respectively, were incubated at ratios of 100/0, 75/25, 50/50, and 25/75 %. Each of these

mixtures was incubated at varying bulk tau levels. Isoform mixtures were incubated in assembly buffer, including 100 μM thiazine red, for 24 hours. Samples were prepared for electron microscopy as described above and total filament length for each sample was determined. Resultant total length was then plotted against bulk tau concentration and the critical concentration for each isoform ratio was calculated ± the standard deviation as described above. These values were then compared to the expected results assuming no isoform dominance.

3.2.8 Pairwise comparisons

To fully delineate the effects of individual exons on aggregation propensity, off and on rate pairwise comparisons were made between isoforms differing in any one exon. Comparisons were expressed as a ratio (R) between critical concentrations, and on or off rates of the isoforms. Pairwise comparisons were made between N0R3/N0R4, N1R3/N1R4 and N2R3/N2R4 for exon 10; between N0R3/N1R3 and N0R4/N1R4 for exon 2; between N1R3/N2R3 and N1R4/N2R4 for exon 3.

3.2.9 Statistics

To determine the significance of these results a “” test was performed using the program JMP 6. The standard error of the mean was used along with R and the value 1.00 to calculate the “Z score” or the “Z stat” which was then used to estimate the *p* value. This provides an estimate of how the R value is different than 1.00 which was

considered to be as no effect. A *p* value of less than 0.05 was considered to be significant.

3.3 Results

3.3.1 Inducer selected for the heterogeneous nucleation of tau

Tau protein does not fibrillize spontaneously *in vitro*. The process requires inducers. By far, many compounds have been used as inducers in tau fibrillization pathway. To study the fibrillization properties of all six tau isoforms, I need to find an inducer that can induce all isoforms to form filaments. No previous studies have successfully shown the use of an inducer that works on six of tau isoforms and their filaments side by side (King, Gamblin et al. 2000). A fatty acid called arachidonic acid (AA) was used as inducer in tau assembly assay. EM photos showed that only isoforms N2R4 and N1R4 formed satisfying filaments. Isoforms N2R3 and N1R3 formed only a few filaments. While isoforms N0R4 and N0R3 formed no filaments (**Figure 3.2**).This result showed that AA cannot be used to induce all isoforms to form filament in vitro which means isoforms N0R4 and N0R3 require much higher critical concentrations than the rest of isoforms when AA is used as inducers. We need to use much more efficient inducers.

3.3.2 Six tau isoforms form filaments under physiological conditions

A small molecular dye called Thiazine-Red (TR) successfully induced the filament formation on all six tau isoforms. They are anionic planar aromatic dyes known to bind

β-sheet structure and used for stain AD lesions *in situ* such as Congo Red, thiazine red, and ThS. Comparing with previous inducers of anionic surfactants and microspheres, dyes induced tau aggregation in their monomer state, supported fibrillization at critical concentrations as low as 200 nM (well within the physiological range), and induced protein aggregation with near homogeneous nucleation kinetics. TR not only have induce all isoforms to form filaments, but also lowered down the critical concentrations of tau. So the protein concentrations used *in vitro* is close to the physiological levels of tau (1 – 10 M) (Drubin, Feinstein et al. 1985; Khatoon, Grundke-Iqbal et al. 1992; Chirita and Kuret 2004) *in vivo*. TR made it possible to study the fibrillization of six isoforms side by side.

EM photos showed that isoform filaments morphology differed a great deal in terms of relative numbers and lengths. N0R3 and N0R4 formed very short, straight, and densely distributed filaments. However, N2R3 and N1R3 formed very long and twisted filaments. Filaments formed by N2R4 and N1R4 are moderate long and evenly scattered (**Figure 3.3**).

Figure 3.4 is group of EM pictures showing the total tau filaments formed in each reaction is propotional to the enitial amount of tau concentration in reaction. The higher tau concentrations used, the greater number and lengthes of tau filaments were formed.

3.3.3 Alternatively spliced exons affect critical concentration

Utilizing thiazine red, all tau isoforms were induced to form filaments. The critical concentration was determined for each and pairwise comparisons were performed.

Critical concentration reflects both the minimal concentration, which will support filament formation and the total amount of unincorporated monomer in solution at equilibrium. Therefore, a lowered critical concentration indicates that a greater proportion of the bulk protein is incorporated into filaments. From lowest to highest, the rank order of isoform critical concentrations is htau N1R4, N2R4, N0R4, N1R3, N2R3, and N0R3 (**Figure 3.5B**). All isoforms containing four microtubule binding repeats have critical concentrations below those with three. Statistical analysis revealed that inclusion of exon 10 lowers the critical concentration approximately six fold ($p<0.001$). Thus, isoforms containing exon 10 aggregate, on average, at six fold lower concentrations than those without (**Figure 3.5C**). Similarly, exon 2 exerts its effect by decreasing the critical concentration two fold ($p<0.001$). In contrast, inclusion of exon 3 raised the critical concentration by approximately 30% ($p<0.001$). This result indicates that the presence of exon 3 exerts a destabilizing influence on the filaments.

3.3.4 Inclusion of exon 10 results in lowered dissociation rates

Variations in critical concentration result from differences in the elementary rate constants, k_{off} and k_{on}. Dissociation rates were determined for each individual isoform by plotting total filament length post-dilution as a function of time. This yields a pseudo zero order curve representing the apparent rate constant k_{app}. This value was then used to calculate k_{off}. Dissociation rates reflect the relative stability of the filaments. Consistent with critical concentration results, 4R isoforms have a three fold lower k_{off} than the 3R isoforms ($p<0.005$), indicating that the presence of exon 10 greatly stabilizes mature

filaments (**Figure 3.6A**). of exons 2 and 3 did not result in a significant change in the rate of dissociation.

3.3.5 Exons 2 and 10 double the rate of association

The association rate constant, $k_{on,}$ was calculated using Equation 2, the k_{off}, and K_{crit} values for each isoform with the associated error statistically propagated (**Figure 3.6B**). Again utilizing pairwise comparisons, the presence of exon 10 was found to increase the rate of association, on average, two fold ($p<0.05$). Addition of exon 2 increases k_{on} by two fold, thus explaining its affect on critical concentration. Inclusion of exon 3 resulted in an approximately 30% decrease in association rate; however it was not statistically significant for one of the two pairwise comparisons.

3.3.6 Isoform structure influences nucleation rate

All isoforms were incubated at constant supersaturation (critical concentration + 0.3μM) and the polymerization time course was followed by electron microscopy (**Figure 3.7A**). The lag time was calculated from the curve by finding the x intercept of a line drawn tangent to the point of inflection. In all cases isoforms containing four microtubule binding repeats had shorter lag times than those with three (**Figure 3.7B**). Analysis of lag time provides an indirect indication of nucleation rate. As stated above, nucleation represents the formation of an energetically unfavorable species and one of the rate limiting steps in the polymerization process. Utilizing pairwise comparisons, it

was determined that inclusion of exon 10 results in a nearly four fold decrease in lag time, with exons 2 and 3 showing no significant effect (**Figure 3.7C**).

3.3.7 N2R4 exerts partial dominance over N0R3

The longest human tau isoform, N2R4, was incubated with N0R3, the shortest, at varying ratios and then assayed for critical concentration. Results were plotted as percentage of htau40 against $1/K_{crit}$ and compared to those expected assuming no dominance (**Figure 3.8**). The data shows that when isoform N2R4 makes up the majority of bulk tau (75-50%) in the reaction critical concentration is lowered relative to the expected values. These findings indicate that more assembly prone splice variants may play a role in recruiting other isoforms into lesions.

3.4 Discussion

The ultimate cause of tau aggregation in Alzheimer's disease and other tauopathies is not clear. Our results show that there is significant different in terms of aggregation kinetics between 3R and 4R tau isoforms. The 4R isoforms have much lowed critical concentration and shorter lag time than 3R tau isoform. Hence, 4R tau is more potent to assemble into filament. When analyzed at the mRNA level, alternative splicing exons make it possible to detect the influence of each exon on polymerization. Addition of exon 2 lowers the critical concentration regardless of the presence or absence of exon 10. It also decreases the nucleation rate, although this effect is diminished in the presence of exon 10. Exon 3 exerts small negative effects on the critical concentration

and the nucleation rate in both 3R and 4R cases. This thermodynamic difference resulting from structure difference can explain why the increased 4R isoform level can lead to FTDP-17 and a great deal of other pathologies mention in chapter one.

One of the major hypotheses regarding tau is that polymerization is the result of hyperphosphorylation. In late stage disease, filamentous tau is phosphorylated at a stoichiometry significantly greater than that of normal tau (Ksiezak-Reding, Liu et al. 1992; Kopke, Tung et al. 1993). However, fetal brain tissue contains tau phosphorylated at nearly the same level, and at many of the same sites as PHF tau, but does not form tangles (Brion, Smith et al. 1993; Kenessey and Yen 1993). Again, these findings can be explained by the differential ability of tau isoforms to aggregate. Alternative splicing of tau is developmentally regulated with only the shortest isoform, htau23, expressed prenatal (Takuma, Arawaka et al. 2003). Studies using phosphorylation mimicry mutants demonstrate that phosphorylation can lower tau's critical concentration (Necula and Kuret 2004). However, our results show that its critical concentration is sufficiently high to create a barrier to aggregation that is not easily surmounted at physiological tau concentrations, even in the presence of phosphorylation.

Two haplotypes (H1 and H2) have been defined for the tau gene, which are described by eight single nucleotide polymorphisms (Baker, Litvan et al. 1999). Homozygosity for the more common H1 haplotype results in a predisposition to progressive supranuclear palsy (PSP) and corticobasal degeneration (CBD). The H1 haplotype is also linked with increases in the proportion of four repeat isoforms (Myers, Pittman et al. 2006). The presence of multiple haplotypes may explain the differential

susceptibility of primates to tauopathies. Chimpanzees are resistant to the development of tau related pathology despite possessing identical amino acid sequences to the human tau gene (Gearing, Rebeck et al. 1994; Holzer, Craxton et al. 2004). Interestingly, it was found that chimpanzees and gorillas have the gene sequence coding for the H2 haplotype. This results in chimpanzees and gorillas expressing a higher proportion of RNA transcripts lacking exon 10 (Holzer, Craxton et al. 2004). Resistance to tau related pathology in chimpanzees is due to over-expression of exon 10 lacking (3R) isoforms with higher critical concentrations, and thus a lower aggregation potential. These results also demonstrate explicitly how the H1 haplotype predisposes carriers to PSP and CBD.

Another unexplained aspect of disease is the selective vulnerability of specific cell populations. One of the areas involved in the genesis of tau pathology very early in the course of disease is the hippocampus. Specifically, the pyramidal neurons of the CA 1 and CA2 regions of the hippocampus typically degenerate in AD and FTDP-17 whereas the granule cells remain unaffected. Granule cells express 3R isoforms alone whereas the pyramidal cells express both 3R and 4R isoforms (Goedert, Spillantini et al. 1989; Yasojima, McGeer et al. 1999). However in FTLD, a disorder characterized by aggregates of 3R isoforms, granule cells are highly affected (Hof, Bouras et al. 1994). Our results indicate that isoform expression may be a key factor in the vulnerability of neurons to the development of pathology in specific conditions. This does not, however, explain why 3R isoforms, which are far less assembly prone, aggregate in Pick's disease. A potential answer for this phenomenon is oxidative stress. In Pick's disease there may be a greater level of oxidation leading to the formation of intermolecular disulfide bonds.

Because 4R tau has two sulfhydryl groups, an intramolecular disulfide bond is possible which would produce and assembly incompetent species, whereas 3R tau contains only one sulfhydryl moiety and thus forms intermolecular disulfide bridges. This would results in dimerization, and may in turn promote nucleation and further polymerization.

These findings indicate that potentially three classes of tauopathy exist differentiated on the basis of isoform involvement. Class 1 would include disorders in which all six tau isoforms are involved. This would include: AD, Down's syndrome, ALS, Neiman-Pick type C, postenchepahlitic parkinsonism, and normal aging. Class II disorders would comprise those involving predominately four repeat isoforms, including PSP, CBD, and genetic forms of FTDP-17 in which intronic or exonic mutations result in a relative increase in 4R isoforms. Progressive supranuclear palsy is a degenerative neurological disorder characterized by ataxia, slowing or inability to generate saccadic eye movements, and axial rigidity. PSP is relatively rare in the United States, with an estimated incidence 1.1 per 100,000, and though the majority of cases are sporadic, a few known pedigrees exist. The disorder is much more common on the islands of Guam and Guadeloupe, located in the Pacific and French West Indies respectively. In both cases the prevalence of the disease has been linked to dietary factors and possibly an interaction with genetics. Corticobasal degeneration is another rare sporadic tauopathy with a slowly progressing late onset course. Finally, Class III disorders are those conditions in which 3R isoforms make up the majority of pathology. In this case only Pick's disease, a rare disorder characterized by progressive dementia and personality

degeneration, and one naturally occurring FTDP-17 mutation ΔK280 have been identified.

The 3R/4R ratio theory dose not fully reveal the underlying mechanism of all tauopathies. Other aspects or factors also contribute to disease formation. One possible aspect is that there is too much tau under pathological conditions. So increased protein concentrations will result in faster aggregation just like amyloid-β and α-synuclein (Singleton, Myers et al. 2004). However, this is not adequate as even supersaturated conditions do not result in tau fibrillization *in vitro*. So tau polymerization needs triggers to turn tau monomer into the assembly competent state. Only at the influence of triggers, tau can assembles via a nucleation dependent pathway with concentration-dependent polymerization rates. Together, Increased tau levels alone dose wholly account for the pathogenesis. Other factors such as posttranslational modifications and oxidative stress may also play a role.

The unevenly expressed tau isoforms in FTDP-17 and other taopathies have revealed that error in tau pre-mRNA processing play a central role in lesion and disease formation. This discovery provides insight into the novel therapeutic strategies for curing diseases. RNA interference (RNAi) has emerged as a potential therapeutic approach for neurodegenerative diseases, particularly those associated with autosomal dominant patterns of inheritance. Several groups have demonstrated efficacy of using viral vectors expressing short hairpin RNA (shRNA) directed against therapeutically relevant genes in mouse models of neurodegenerative diseases, including spinocerebellar ataxia, Amyotrophic Lateral Sclerosis, Huntington's Disease and

amyloidosis (Farah 2007). On the other side, robust researches have been done trying the find the inhibitors for tau aggregation. We therefore continue our search for non-toxic, cellpenetrating inhibitors of tau aggregation, which hold potential for brain penetration. In addition, drugs aiming to reduce tau phosphorylation (GSK3 inhibitors) are about to enter clinical phases of development (Giacobini and Becker 2007).

3.5 Summary

Frontotemporal dementia and parkinsonism linked to chromosome 17 (FTDP-17) is a rarely occurring autosomal-dominant dementia with severe frontotemporal atrophy. Despite substantial neuropathological heterogeneity, the formation of abundant filamentous tau inclusions in neurons and glia is a defining characteristic of FTDP-17 as well as other tauopathies. Recently, mutations on the tau gene have been identified in cases of FTDP-17, demonstrating that genetic deficits in tau can cause neurodegeneration. Thirty-nine exonic and intronic tau mutations have been identified to date. All the intronic mutations exert their pathogenic effects by altering tau mRNA splicing of exon 10 leading to increased level of four-repeat (4R) tau. Normal tau protein is produced, however, the 4R/3R ratio is raised from 1 to 2-3. The underlying mechanism of altered tau isoform ratio leading to disease formation is unknown. Since tau assembles via a nucleation dependent mechanism, by using quantitative electron microscopy, we assessed the nucleation kinetics for 4R and 3R isoforms through the collection of critical concentrations and time courses. Our results show that 4R tau is more pro-fibrillogenic than 3R tau by requiring much lower critical concentration and

possessing higher nucleation efficiency. Moreover, the dominant fibrillogenic potential of 4R over 3R tau is accredited to the relative efficiency of exons 2, 3 and 10 in promoting tau monomer aggregation. Quantitative analysis demonstrates that exon 10 is a much stronger driving force to filament formation than exons 2, and 3. The difference in the aggregation nature between 4R and 3R tau isoforms helps to explain why intronic mutations in tau gene lead to disease formation.

3.6 Figures

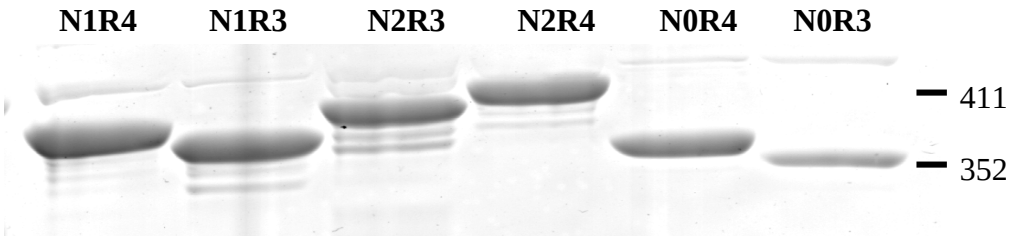

Figure 3.1 Purified tau isoforms in SDS-PAGE gel.

Recombinant histidine-tagged tau proteins were purified. The quality of six tau isoforms was assessed by SDS-PAGE. Sizes of tau isoforms range from 441 to 352 amino acids. The final protein concentrations were calibrated on the basis of optical density by absorbance at 280 nm. Proteins are all diluted in to the same concentrations (2.5 mg/ml) and stored in -20 ºC.

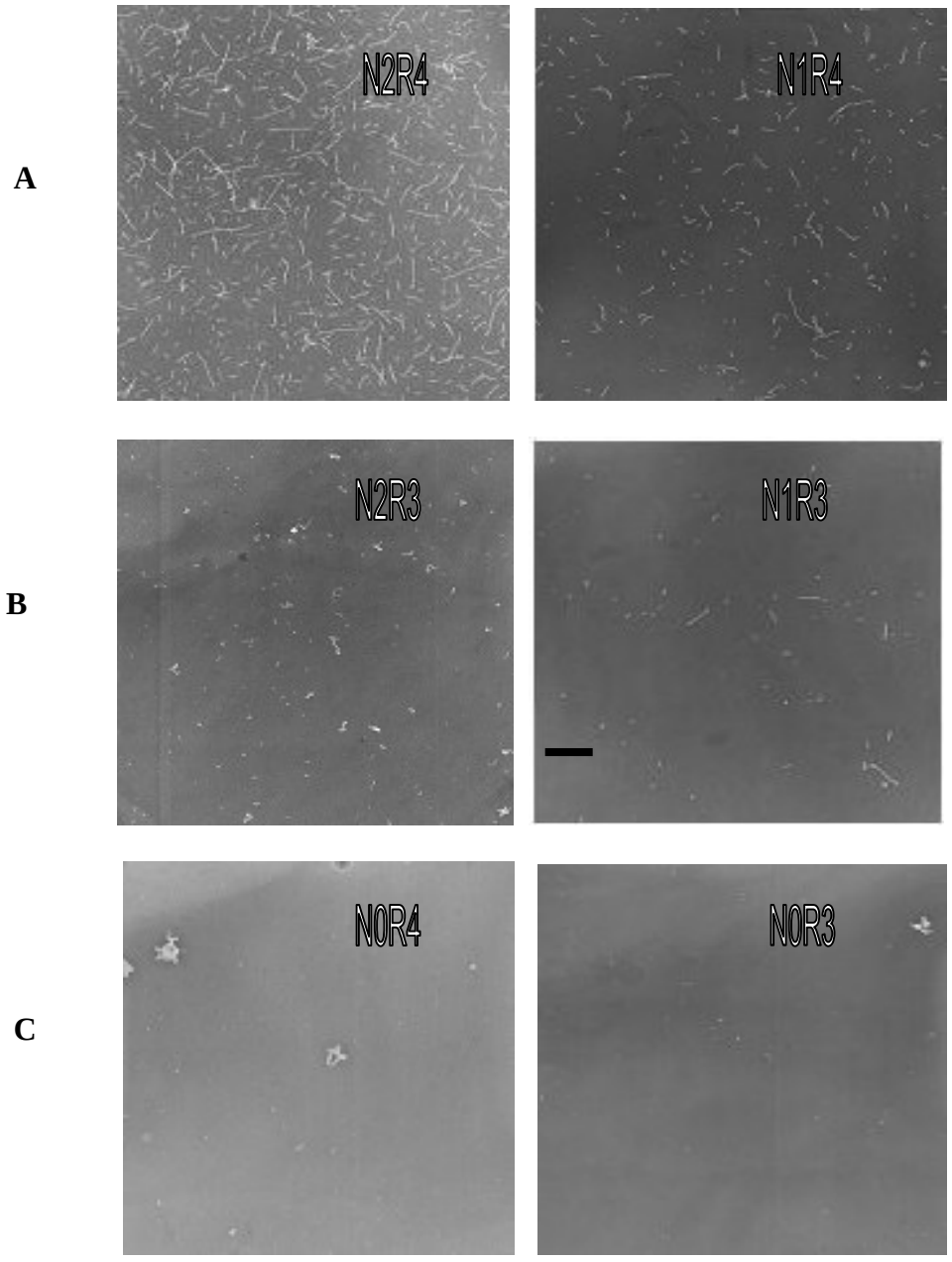

Figure 3.2 Arachidonic Acid induced tau isoform aggregation.

A fatty acid called arachidonic acid (AA) was used as inducer in tau assembly assay. EM photos for each of tau isoform showed significant difference regarding filament formation. **(A)** Isoforms N2R4 and N1R4 formed a large number of filaments. **(B)** Isoforms N2R3 and N1R3 formed only a few filaments. **(C)** Isoforms N0R4 and N0R3 formed no filaments. (scale bar 500nm)

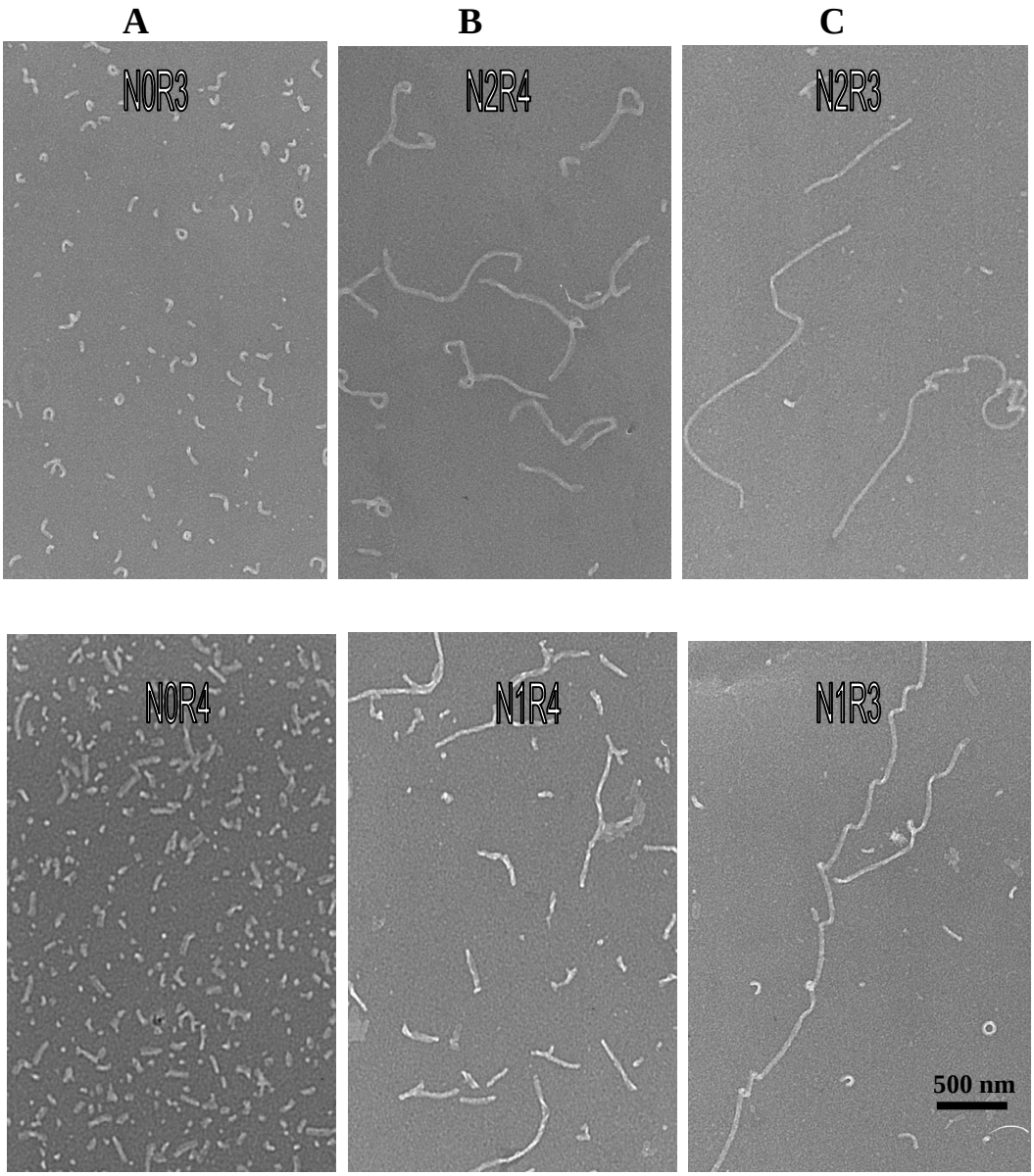

Figure 3.3 Thiazine Red (TR) induced tau isoform aggregation.

Small planar aromatic dye Thianzine Red (TR) successfully induced all six tau isoforms to form filaments *in vitro*. EM photos showed that isoform filaments morphology differed a great deal in terms of relative numbers and lengths.
(A) N0R3 and N0R4 formed very short, straight, and densely distributed filaments.
(B) N2R4 and N1R4 formed moderate long and evenly scattered filaments.
(C) N2R3 and N1R3 formed very long and twisted filaments.

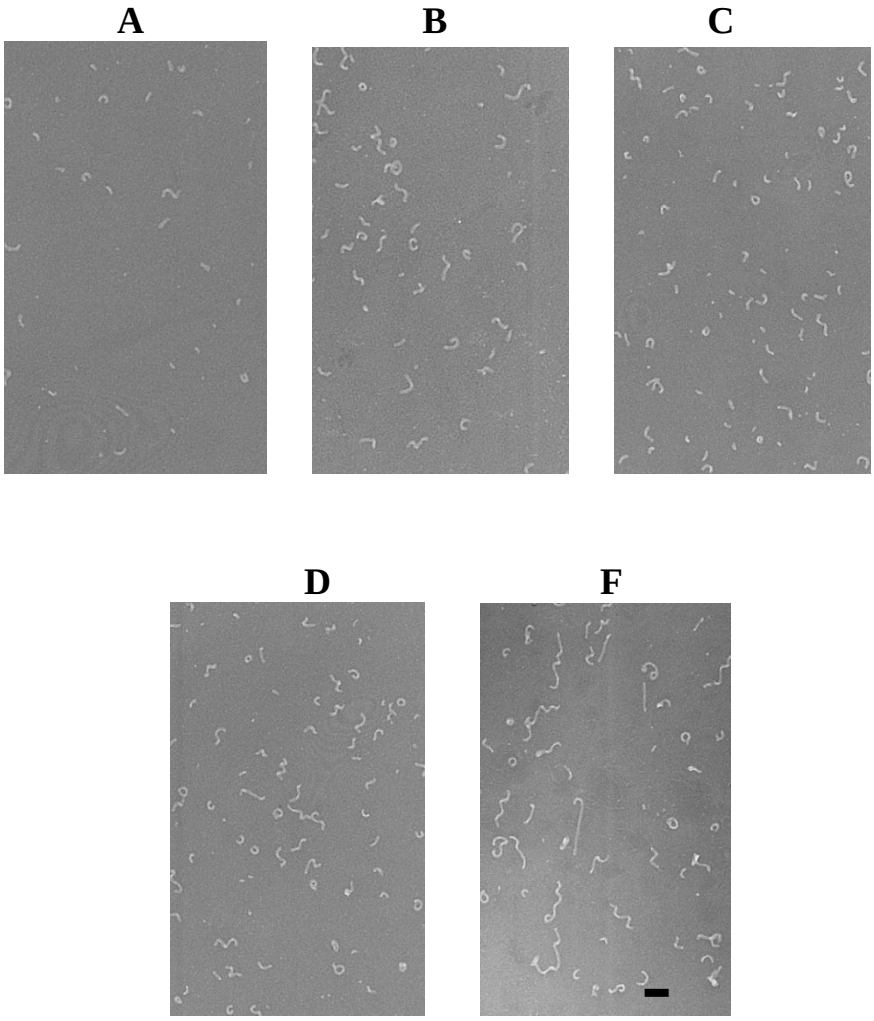

Fig. 3.4 Filaments formed by N0R3 for Critical Concentration (CC) analysis.

Representive EM photos showed Thianzine Red (100 μM) induced aggregation for isoform N0R3. N0R3 tau concentrations added in reactions from A to F are respectively 4.5, 5.0, 5.5, 6.0, 6.5 μM. After incubation for 4 hours at 37°C, aliquots were then stained with uranyl acetate and examined by transmission electron microscopy. **A-F.** Total tau filaments (both filament number and lengh) increased in accordance with the initial tau concentration in reaction. (scale 500nm)

Figure 3.5 Tau isoforms differ in critical concentration.

Tau isoforms 0N3R (○), 1N3R (□), 2N3R (Δ), 0N4R (●), 1N4R (■), and 2N4R (▲) were incubated (24 h at 37°C) in the presence of 100 μM Thiazine red, then assayed for filament formation by electron microscopy. ***A,*** plot of total filament length against bulk protein concentration, where each data point represents the mean ± SD of triplicate determinations and the solid lines represent best fit of the data points to linear regression. The abscissa intercept was taken as the critical concentration (K_{crit}). K_{crit} depended on the presence or absence of alternatively spliced segments. ***B,*** replot of data from Panel A, where each bar represents the average contribution of segments encoded by Exons 2 (*gray bar*), 3 (*white bar*) or 10 (*black bar*) to K_{crit} relative to background (*dashed line*). Averages were calculated from pairwise comparisons of isoforms 1N3R/0N3R and 1N4R/0N4R (Exon 2), 2N3R/1N3R and 2N4R/1N4R (Exon 2), and 0N4R/0N3R, 1N4R/1N3R, and 2N4R/2N3R (Exon 2) ± propagated SE. The presence of either Exon 2 or 10 lowered K_{crit}, whereas K_{crit} rose in the presence of Exon 3. $**p <$ 0.01; n.s. $p > 0.05$ when compared to background.

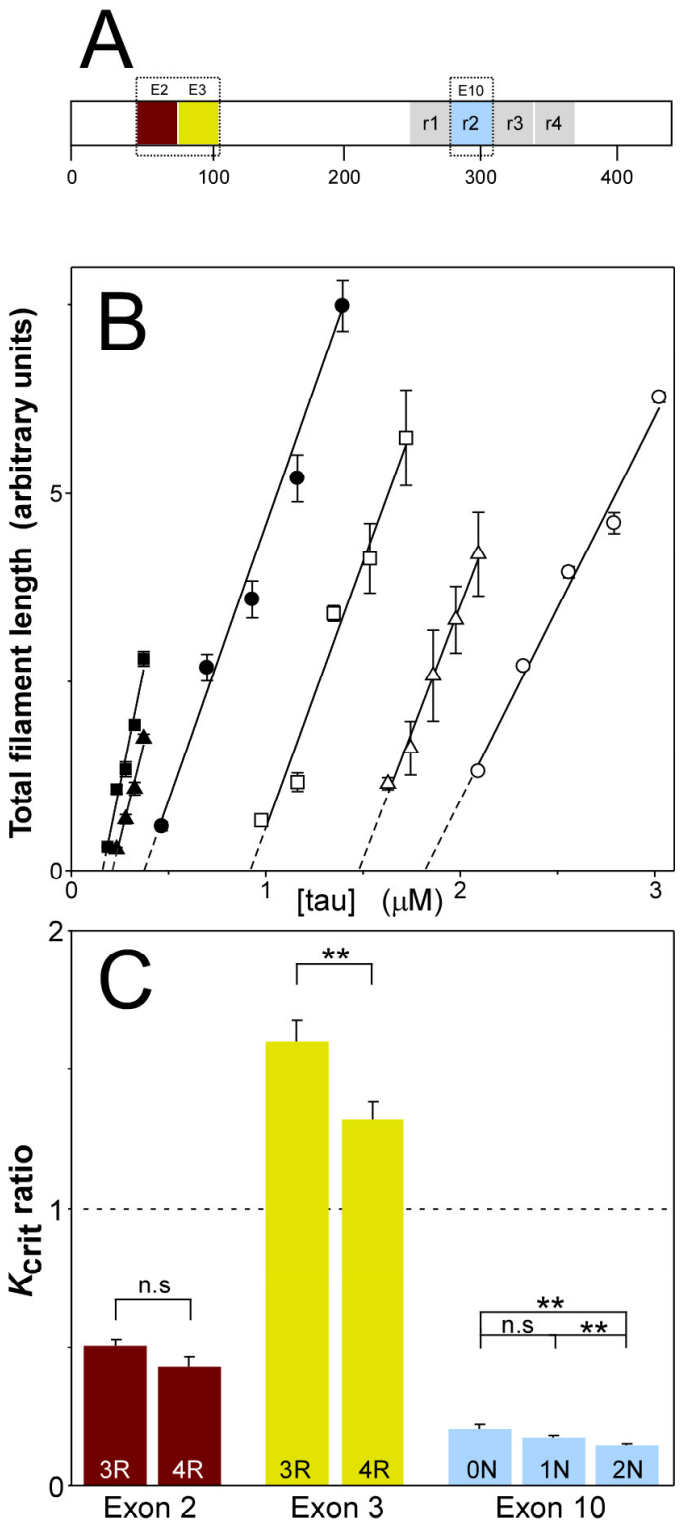
A
E2
E3
E10
r1
r2
r3
r4
0
100
200
300
400
B
Total filament length (arbitrary units)
5
0
0
1
[tau] (μM)
2
3
C
2
1
0
**
n.s
**
n.s
**
3R
4R
3R
4R
0N
1N
2N
Exon 2
Exon 3
Exon 10
Kcrit ratio

Figure 3.6 Extension association and dissociation rates constants vary by tau isoform.

A, Dissociation rate constants (k_{e-}) were measured from filaments composed of 3R (*white bars*) and 4R (*black bars*) tau isoforms ± SE, and then ***B***, used in conjunction with measured K_{crit} values to estimate association rate constants (k_{e+}) mediating filament extension. ***C***, the contribution of individual tau segments to k_{e-} and k_{e+} was then calculated and averaged ± SE from pair-wise comparisons relative to background (*dashed line*) as described in **Fig. 1**. Exon 2 depressed K_{crit} by selectively increasing k_{e+}, whereas Exon 10 both increased k_{e+} and decreased k_{e-}. In contrast, Exon 3 increased K_{crit} by decreasing k_{e+}. See text for details. $**p < 0.01$ when compared to background.

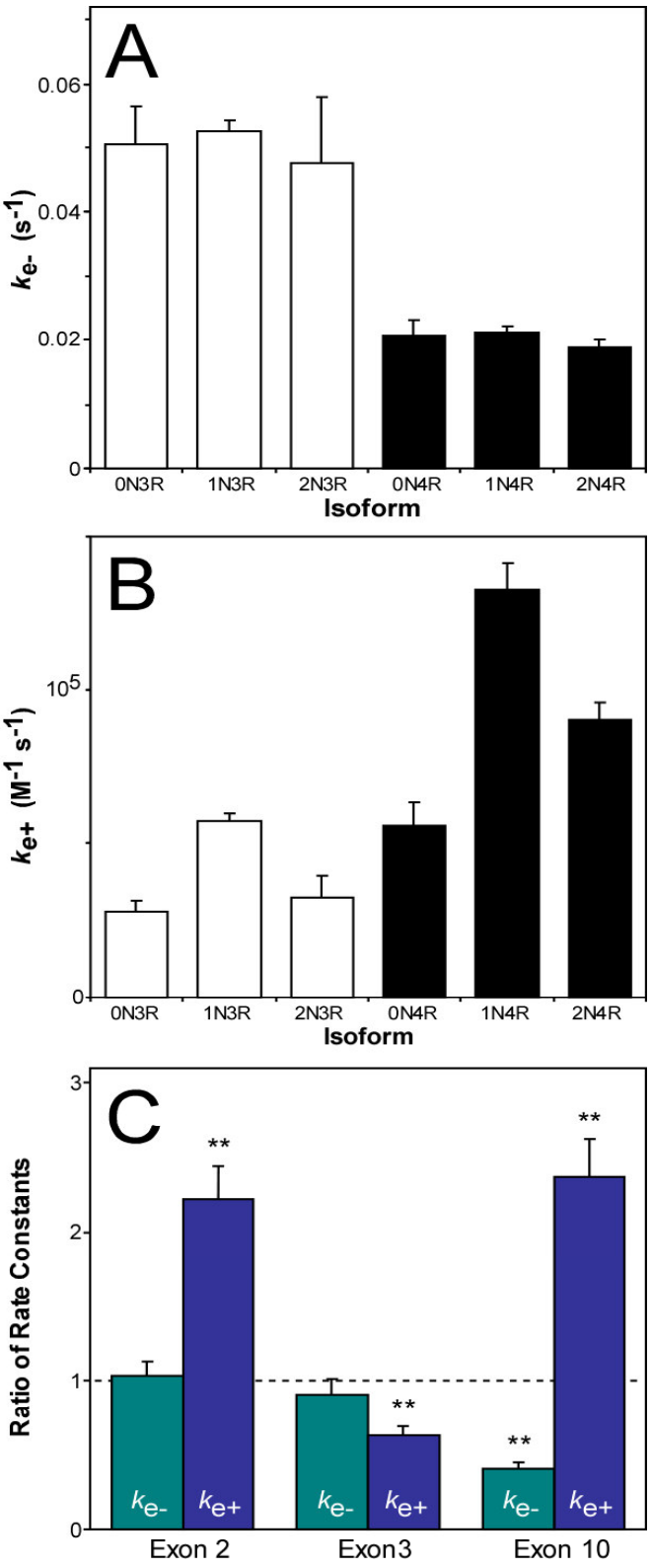
A
0.06
0.04
0.02
0
k_{e-} (s^{-1})
0N3R
1N3R
2N3R
0N4R
1N4R
2N4R
Isoform
B
10^5
0
k_{e+} (M^{-1} s^{-1})
0N3R
1N3R
2N3R
0N4R
1N4R
2N4R
Isoform
C
3
2
1
0
Ratio of Rate Constants
**
**
**
k_{e-}
k_{e+}
k_{e-}
k_{e+}
k_{e-}
k_{e+}
Exon 2
Exon3
Exon 10

Figure 3.7 Effect of alternative splicing on aggregation time course.

A, tau isoforms 0N3R (○), 1N3R (□), 2N3R (Δ), 0N4R (●), 1N4R (■), and 2N4R (▲) were incubated (37°C) at constant supersaturation (*i.e.*, 0.3 μM above K_{crit}) in the presence of 100 μM Thiazine red, and then assayed for filament formation as a function of time. Each data point represents average filament lengths/field calculated from triplicate electron microscopy images whereas each normalized curve represents best fit of the data points to a three parameter Gompertz growth function (30). ***B***, lag times ± SE calculated from each Gompertz regression (3R, *white bars*; 4R, *black bars*). Three-repeat isoforms aggregated with longer lag times than four-repeat isoforms. ***C***, the contribution of individual tau segments to lag time was then calculated and averaged ± SE from pair-wise comparisons relative to background (*dashed line*) as described in **Fig. 1**. The presence of Exon 10 decreased lag time. $^{**}p < 0.01$ when compared to background.

.

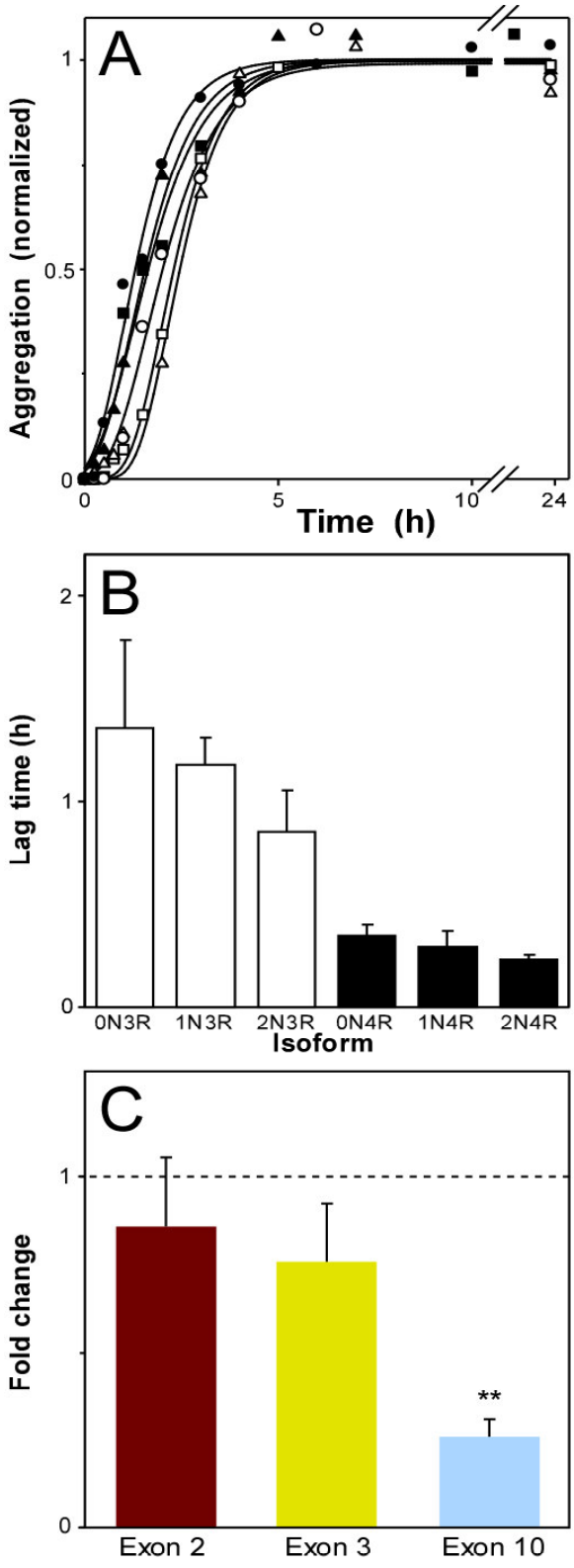
A
Aggregation (normalized)
1
0.5
0
0
5
10
24
Time (h)
B
Lag time (h)
2
1
0
0N3R
1N3R
2N3R
0N4R
1N4R
2N4R
Isoform
C
Fold change
1
0
**
Exon 2
Exon 3
Exon 10

Figure 3.8 4R tau is dominant over 3R tau.

Tau isoforms 2N4R and 0N3R were incubated together (24 h at 37^{o}C) in 3:1 (♦), 1:1 (◊), and 1:3 (▽) ratios in the presence of 100 μM thiazin red, then subjected to filament length measurements by electron microscopy. ***A,*** plot of total filament length against bulk protein concentration, where each data point represents the mean ± SD of triplicate determinations and the solid lines represent best fit of the data points to linear regression. The abscissa intercept was taken as K_{crit}. ***B***, replot of data from Panel A, where each point represents experimentally determined K_{crit} ± SE at the given isoform ratio, the dashed line represents the boundary prediction of no interaction between isoforms, and the dotted line represents the boundary prediction where interaction is complete and all tau behaves as 0N4R. Under these conditions, 2N4R tau is dominant and drives a portion of 0N3R tau into aggregates. $*p < 0.05$; $**p < 0.01$ compared to boundary predictions.

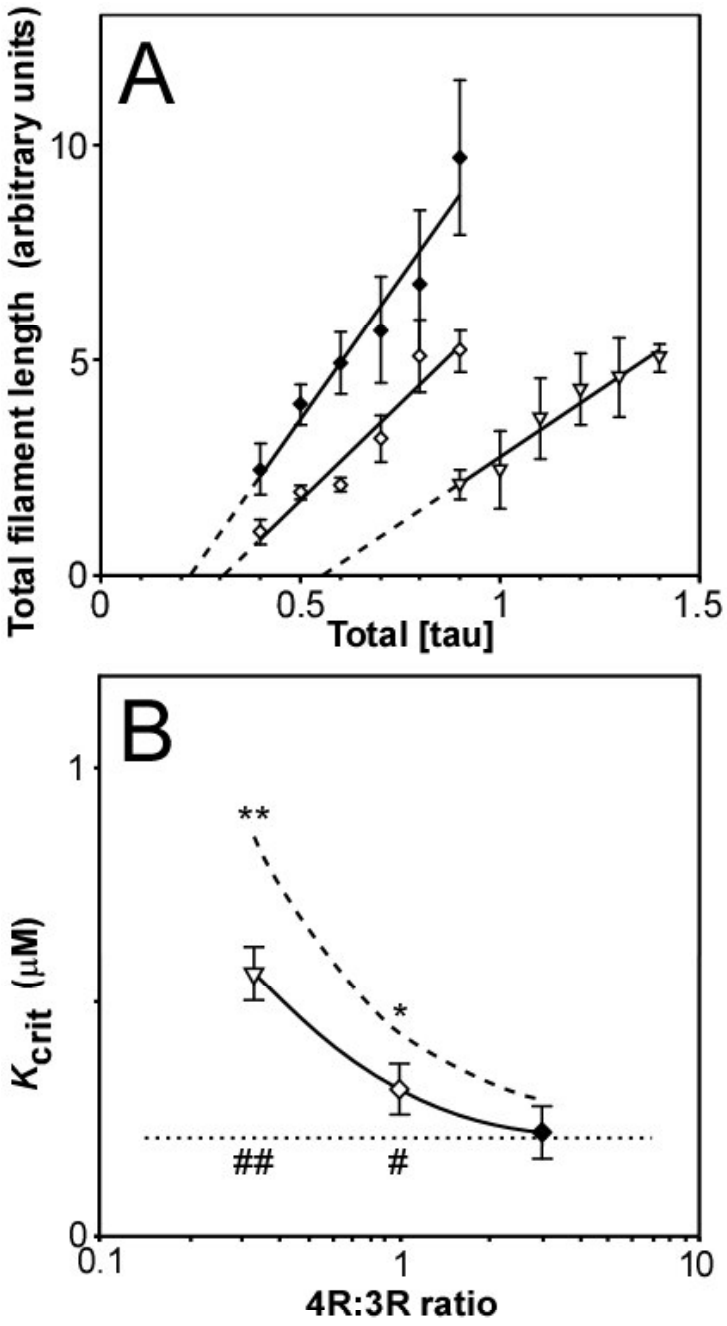
A
Total filament length (arbitrary units)
10
5
0
0
0.5
1
1.5
Total [tau]
B
1
0
0.1
1
10
K_{crit} (μM)
**
*
##
#
4R:3R ratio

CHAPTER 4

4 SUMMARY AND FUTURE WORK

Tau is as an elongated molecule (about 35-50 nm long) without recognizable secondary structure. There are six isoforms in the human brain which are generated from a single gene by alternative splicing, ranging in size from 352-441 amino acids**.** The best-known function of tau is its involvement in microtubule assembly and stabilization. Tau can promote of assembly and stabilization of microtubular network, which is essential for normal axonal transport of vesicles within the neuron.

MAP tau is a protein whose expression is developmentally regulated. In fetal brain only a single isoform exists, corresponding to the smallest of the tau isoforms. In adult human brain six isoforms are produced from a single gene by alternative splicing of exons 2, 3, 10. Exon 10 encodes the fourth microtubule binding domain on tau protein. Thus the isoforms can be classified as 3R tau and 4R tau.

Tau appears to be enriched in axons, and it is the inappropriate hyperphosphorylation of tau in AD and many other tauopathies that contributes towards NFTs development. Filamentous tau deposits in neurons or glia cells constitute a defining characteristic of several neurodegenerative diseases collectively called tauopathies. They include Alzheimer's disease, Pick's disease, CBD, PSP, AGD, and FTDP-17. The discovery of tau intronic mutations leads to the development of FTDP-17. This provides the evidence that abnormalities in tau function or expression are

sufficient to cause filamentous aggregation of hyperphosphorylated tau and neurodegeneration similar to that seen in sporadic tauopathies.

Tau fibrillization pathway *in vitro* follows the nucleation-elongation model. The kinetics of nucleation-dependent polymerization is characterized by two important factors: critical concentration and elongation lag time. Obtaining and comparing the kinetic of the 4R vs. 3R tau isoforms is of significant importance in the understanding the mechanism underlying pathological tau fibrillization. Six tau isoforms was purified and a solution-based tau assembly essay was carried. A Small anionic planar aromatic dyes thiazine red was used as inducer to supported fibrillization at critical concentrations as low as 200 nM. By using quantitative electron microscopy, we investigated the aggregation kinetics for the six tau isoforms. The relative critical concentrations and lag time for each of the isoforms were compared. The dissociation rate k_{off} and the association rate k_{on} were calculated for each isoform. Out results show that alternatively spliced exons effect critical concentration as well as the rate of polymerization. Inclusion of exon 10 and exon 2 results in lowered Critical concentration and greatly accelerated the polymerization. Exon 3 has a small negative effect on aggregation kinetics. A mixture of 4R and 3R experiment was carried out with mixed N2R4 and N0R3. Result showed the longest isoform exerts a dominant effect in polymerization over the shortest isoform.

Although increasing evidence supports that alterations of tau may directly cause neuronal degeneration and cell death, the mechanisms, which render tau to become a toxic agent are still unclear. Our results privide significant biologically implications in

the pathogenesis of many tauopathies by explaining why increased 4R tau ratio is sufficient to cause neurodegenerative diseases. Neurons require a precise stoichiometry of tau isoforms to keep normal functions and 4R and 3R tau may bind to different sites on microtubules and have different potential in binding and stablizing them. Genetic error occoring at the pre-mRNA thythesis lead to overproduction of 4R tau isoforms. The eccess of 4R tau may result in an excess of tau over available binding sites on microtubules. This abundance may lead to accumulation of unassociated tau. Unbound tau aggregates and is phosphorylated and precipitated into filaments in neuron. Over long period of time, large amounts of toxic tau filaments further forms NFTs. Without the binding of tau protein, microtubules will “crash down” and depolarized. This will trigger a series of abnormalities in intracellular signaling and neuronal trafficking. Neurons are unable to maintain their morphology and function and eventually undergo neuronal death.

In human, tau protein undergoes several posttranslational modifications: such as phosphorylation, truncation, nitration, glycation, glycosylation, ubiquitination and polyaminations. When these modifications are disturbed, they play a serious role during the pathogenesis. Phosphorylated tau has reduced capability in binding to microtubules and hyperphosphorylation together with truncation contributes to the formation of pathological tau filaments. We also found that phosphorylation of tau can also enhance tau aggregation *in vitro* (Necula and Kuret 2004). This leads to destabilization of microtubular network and subsequent impairment of microtubule associated axonal transport. The abnormal hyperphosphorylation not only results in the loss of tau

function of promoting assembly and stabilizing microtubules but also in a gain of a toxic function whereby the pathological tau sequesters normal tau, MAP1A/MAP1B and MAP2, and causes inhibition and disruption of microtubules (Iqbal, Alonso Adel et al. 2005).

The hyperphosphorylation of tau results both from an imbalance between the activities of tau kinases and tau phosphatases and as well as changes in tau's conformation which affect its interaction with these enzymes. CK1 has been indicated as a candidate enzyme for tau hyperphosphorylation. Our RT-PCR results have demonstrated that CK1 isoforms mRNA is upregulated in AD hippocampus versus control cases, especially Ck1-delta that was elevated up to 13-fold and gamma 2 was elevated up to 4-fold. The rest of CK1 kinases (alpha, gamma1, gamma2 and epsilon) do not shown to have a difference between AD and control groups. The elevated mRNA expression level in AD suggests that CK1 isoform delta and gamma 2 are highly involved in AD pathogenesis.

Because the number of tau inclusions and their regional distribution correlate with clinical symptoms, inhibition of tau aggregation or filament formation in neurons or glial cells may prevent neurodegeneration. So screening potent inhibitors for tau aggregation is another important job in future for the potencial treatment of tauopathies (del, Li et al. 2008). Other therapeutic approaches are aims to inhibit tau phosphorylation and aggregation or to dissolve preexisting tau aggregates. Further experimental therapy strategies include the enhancement of tau clearance by activation of proteolytic, proteasomal, or autophagosomal degradation pathways or anti-tau

directed immunotherapy (Schindowski, Belarbi et al. 2008). In several tauopathies there is a shift toward four-repeat tau isoforms, and interference with the splicing machinery to decrease four-repeat splicing might be another therapeutic option. Hyperphosphorylated tau does not bind microtubules, leading to microtubule instability and transport impairment. Pharmacological stabilization of microtubule networks might counteract this effect and serves as a therapeutic option (Friedhoff, Schneider et al. 1998).

.

LIST OF REFERENCES

Aarskog, N. K. and C. A. Vedeler (2000). "Real-time quantitative polymerase chain reaction. A new method that detects both the peripheral myelin protein 22 duplication in Charcot-Marie-Tooth type 1A disease and the peripheral myelin protein 22 deletion in hereditary neuropathy with liability to pressure palsies." Hum Genet **107**(5): 494-8.

Abeliovich, A., Y. Schmitz, et al. (2000). "Mice lacking alpha-synuclein display functional deficits in the nigrostriatal dopamine system." Neuron **25**(1): 239-252.

Agarwal-Mawal, A. and H. K. Paudel (2001). "Neuronal Cdc2-like protein kinase (Cdk5/p25) is associated with protein phosphatase 1 and phosphorylates inhibitor-2." J Biol Chem **276**(26): 23712-8.

Andreadis, A. (2005). "Tau gene alternative splicing: expression patterns, regulation and modulation of function in normal brain and neurodegenerative diseases." Biochim Biophys Acta **1739**(2-3): 91-103.

Avila, J., et al. (2004). "Role of Tau Protein in Both Physiological and Pathological Conditions." Physiol. Rev. **84**(2): 361-384.

Avila, J. and F. Hernandez (2007). "GSK-3 inhibitors for Alzheimer's disease." Expert Rev Neurother **7**(11): 1527-33.

Avila*, F. H. n. a. J. (2007). "Tauopathies." Cellular and Molecular Life Sciences **64**: 2219 – 2233.

Baker, M., I. Litvan, et al. (1999). "Association of an extended haplotype in the tau gene with progressive supranuclear palsy." Hum Mol Genet **8**(4): 711-5.

Bancher, C., C. Brunner, et al. (1989). "Accumulation of abnormally phosphorylated tau precedes the formation of neurofibrillary tangles in Alzheimer's disease." Brain Res. **477**(1-2): 90-99.

Barghorn, S. and E. Mandelkow (2002). "Toward a unified scheme for the aggregation of tau into Alzheimer paired helical filaments." Biochemistry **41**(50): 14885-96.

Beuve, M., L. Sempe, et al. (2007). "A sensitive one-step real-time RT-PCR method for detecting Grapevine leafroll-associated virus 2 variants in grapevine." J Virol Methods **141**(2): 117-24.

Braak, E., H. Braak, et al. (1994). "A sequence of cytoskeleton changes related to the formation of neurofibrillary tangles and neuropil threads." Acta Neuropathol. (Berl.) **87**(6): 554-567.

Braak, H. and E. Braak (1991). "Neuropathological stageing of Alzheimer-related changes." Acta Neuropathol. (Berl.) **82**(4): 239-259.

Brion, J. P., C. Smith, et al. (1993). "Developmental changes in tau phosphorylation: fetal tau is transiently phosphorylated in a manner similar to paired helical filament-tau characteristic of Alzheimer's disease." J Neurochem **61**(6): 2071-80.

Buee, L., T. Bussiere, et al. (2000). "Tau protein isoforms, phosphorylation and role in neurodegenerative disorders." Brain Res Brain Res Rev **33**(1): 95-130.

Carmel, G., B. Leichus, et al. (1994). "Expression, purification, crystallization, and preliminary x-ray analysis of casein kinase-1 from Schizosaccharomyces pombe." J Biol Chem **269**(10): 7304-9.

Carmel, G., E. M. Mager, et al. (1996). "The structural basis of monoclonal antibody Alz50's selectivity for Alzheimer's disease pathology." J. Biol. Chem. **271**(51): 32789-32795.

Chen, X., T. Huang, et al. (2008). "Involvement of calpain and p25 of CDK5 pathway in ginsenoside Rb1's attenuation of beta-amyloid peptide25-35-induced tau hyperphosphorylation in cortical neurons." Brain Res **1200**: 99-106.

Chirita, C., M. Necula, et al. (2004). "Ligand-dependent inhibition and reversal of tau filament formation." Biochemistry **43**(10): 2879-87.

Chirita, C. N., E. E. Congdon, et al. (2005). "Triggers of full-length tau aggregation: a role for partially folded intermediates." Biochemistry **44**(15): 5862-72.

Chirita, C. N. and J. Kuret (2004). "Evidence for an intermediate in tau filament formation." Biochemistry **43**(6): 1704-14.

Chirita, C. N. and J. Kuret (2004). "Evidence for an intermediate in tau filament formation." Biochemistry **43**(6): 1704-1714.

Chirita, C. N., M. Necula, et al. (2003). "Anionic micelles and vesicles induce tau fibrillization in vitro." J Biol Chem **278**(28): 25644-50.

Cho, J. H. and G. V. Johnson (2004). "Glycogen synthase kinase 3 beta induces caspase-cleaved tau aggregation in situ." J Biol Chem **279**(52): 54716-23.

Churcher, I. (2006). "Tau therapeutic strategies for the treatment of Alzheimer's disease." Curr Top Med Chem **6**(6): 579-95.

D'Souza, I., P. Poorkaj, et al. (1999). "Missense and silent tau gene mutations cause frontotemporal dementia with parkinsonism-chromosome 17 type, by affecting multiple alternative RNA splicing regulatory elements." Proc Natl Acad Sci U S A **96**(10): 5598-603.

D'Souza, I. and G. D. Schellenberg (2005). "Regulation of tau isoform expression and dementia." Biochim Biophys Acta **1739**(2-3): 104-15.

Dehmelt, L. and S. Halpain (2004). "Actin and microtubules in neurite initiation: are MAPs the missing link?" J Neurobiol **58**(1): 18-33.

Dehmelt, L. and S. Halpain (2005). "The MAP2/Tau family of microtubule-associated proteins." Genome Biol **6**(1): 204.

del, C. A. A., B. Li, et al. (2008). "Mechanism of tau-induced neurodegeneration in Alzheimer disease and related tauopathies." Curr Alzheimer Res **5**(4): 375-84.

DiTella, M., F. Feiguin, et al. (1994). "Microfilament-associated growth cone component depends upon Tau for its intracellular localization." Cell Motil Cytoskeleton **29**(2): 117-30.

Dos Santos, H. W., T. R. Poloni, et al. (2008). "A simple one-step real-time RT-PCR for diagnosis of dengue virus infection." J Med Virol **80**(8): 1426-33.

Drubin, D. G., S. C. Feinstein, et al. (1985). "Nerve growth factor-induced neurite outgrowth in PC12 cells involves the coordinate induction of microtubule assembly and assembly-promoting factors." J. Cell Biol. **101**(5 Pt 1): 1799-1807.

Dubois, T., S. Howell, et al. (2002). "Identification of casein kinase Ialpha interacting protein partners." FEBS Lett **517**(1-3): 167-71.

Dubois, T., P. Kerai, et al. (2001). "Casein kinase I associates with members of the centaurin-alpha family of phosphatidylinositol 3,4,5-trisphosphate-binding proteins." J Biol Chem **276**(22): 18757-64.

Dunckley, T., T. G. Beach, et al. (2006). "Gene expression correlates of neurofibrillary tangles in Alzheimer's disease." Neurobiol Aging **27**(10): 1359-71.

Escutenaire, S., N. Mohamed, et al. (2007). "SYBR Green real-time reverse transcription-polymerase chain reaction assay for the generic detection of coronaviruses." Arch Virol **152**(1): 41-58.

Etienne, M. A., N. J. Edwin, et al. (2007). "Beta-amyloid protein aggregation." Methods Mol Biol **386**: 203-25.

Ezquerra, M., C. Gaig, et al. (2007). "Tau and saitohin gene expression pattern in progressive supranuclear palsy." Brain Res **1145**: 168-76.

Farah, M. H. (2007). "RNAi silencing in mouse models of neurodegenerative diseases." Curr Drug Deliv **4**(2): 161-7.

Feinstein, S. C. and L. Wilson (2005). "Inability of tau to properly regulate neuronal microtubule dynamics: a loss-of-function mechanism by which tau might mediate neuronal cell death." Biochim Biophys Acta **1739**(2-3): 268-79.

Ferrer, I., R. Blanco, et al. (2001). "Phosphorylated map kinase (ERK1, ERK2) expression is associated with early tau deposition in neurones and glial cells, but not with increased nuclear DNA vulnerability and cell death, in Alzheimer disease, Pick's

disease, progressive supranuclear palsy and corticobasal degeneration." Brain Pathol **11**(2): 144-58.

Ferrer, I., G. Santpere, et al. (2008). "Argyrophilic grain disease." Brain **131**(Pt 6): 1416-32.

Flajolet, M., G. He, et al. (2007). "Regulation of Alzheimer's disease amyloid-beta formation by casein kinase I." Proc Natl Acad Sci U S A **104**(10): 4159-64.

Freund, V., F. Pons, et al. (2002). "Upregulation of nerve growth factor expression by human airway smooth muscle cells in inflammatory conditions." Eur Respir J **20**(2): 458-63.

Friedhoff, P., A. Schneider, et al. (1998). "Rapid assembly of Alzheimer-like paired helical filaments from microtubule-associated protein tau monitored by fluorescence in solution." Biochemistry **37**(28): 10223-30.

Friedhoff, P., M. von Bergen, et al. (1998). "A nucleated assembly mechanism of Alzheimer paired helical filaments." Proc Natl Acad Sci U S A **95**(26): 15712-7.

Gales, L., L. Cortes, et al. (2005). "Towards a structural understanding of the fibrillization pathway in Machado-Joseph's disease: trapping early oligomers of non-expanded ataxin-3." J Mol Biol **353**(3): 642-54.

Gasparini L, T. B., Spillantini MG (2007). "Frontotemporal dementia with tau pathology." Neurodegener Dis **4**(2-3): 236-53.

Gearing, M., G. W. Rebeck, et al. (1994). "Neuropathology and apolipoprotein E profile of aged chimpanzees: implications for Alzheimer disease." Proc Natl Acad Sci U S A **91**(20): 9382-6.

Giacobini, E. and R. E. Becker (2007). "One hundred years after the discovery of Alzheimer's disease. A turning point for therapy?" J Alzheimers Dis **12**(1): 37-52.

Goedert, M., M. G. Spillantini, et al. (1989). "Cloning and sequencing of the cDNA encoding an isoform of microtubule-associated protein tau containing four tandem repeats: differential expression of tau protein mRNAs in human brain." Embo J **8**(2): 393-9.

Graham, D. A., C. Taylor, et al. (2006). "Development and evaluation of a one-step real-time reverse transcription polymerase chain reaction assay for the detection of salmonid alphaviruses in serum and tissues." Dis Aquat Organ **70**(1-2): 47-54.

Gray, E. G., M. Paula-Barbosa, et al. (1987). "Alzheimer's disease: paired helical filaments and cytomembranes." Neuropathol. Appl. Neurobiol. **13**(2): 91-110.

Gross, S. D. and R. A. Anderson (1998). "Casein kinase I: spatial organization and positioning of a multifunctional protein kinase family." Cell Signal **10**(10): 699-711.

Gross, S. D., C. Simerly, et al. (1997). "A casein kinase I isoform is required for proper cell cycle progression in the fertilized mouse oocyte." J Cell Sci **110 (Pt 24)**: 3083-90.

Gutala, R. V. and P. H. Reddy (2004). "The use of real-time PCR analysis in a gene expression study of Alzheimer's disease post-mortem brains." J Neurosci Methods **132**(1): 101-7.

Hanger, D. P., H. L. Byers, et al. (2007). "Novel phosphorylation sites in tau from Alzheimer brain support a role for casein kinase 1 in disease pathogenesis." J Biol Chem **282**(32): 23645-54.

Harper, J. D. and P. T. Lansbury, Jr. (1997). "Models of amyloid seeding in Alzheimer's disease and scrapie: mechanistic truths and physiological consequences of the time-dependent solubility of amyloid proteins." Annu Rev Biochem **66**: 385-407.

Harrison-Bernard, L. M., S. S. El-Dahr, et al. (1999). "Regulation of angiotensin II type 1 receptor mRNA and protein in angiotensin II-induced hypertension." Hypertension **33**(1 Pt 2): 340-6.

Hartig, W., C. Klein, et al. (2000). "Abnormally phosphorylated protein tau in the cortex of aged individuals of various mammalian orders." Acta Neuropathol (Berl) **100**(3): 305-12.

Hernandez, F. and J. Avila (2007). "Tauopathies." Cell Mol Life Sci **64**(17): 2219-33.

Hof, P. R., C. Bouras, et al. (1994). "Quantitative neuropathologic analysis of Pick's disease cases: cortical distribution of Pick bodies and coexistence with Alzheimer's disease." Acta Neuropathol (Berl) **87**(2): 115-24.

Hogg, M., Z. M. Grujic, et al. (2003). "The L266V tau mutation is associated with frontotemporal dementia and Pick-like 3R and 4R tauopathy." Acta Neuropathol. (Berl.) **106**(4): 323-336.

Holzer, M., M. Craxton, et al. (2004). "Tau gene (MAPT) sequence variation among primates." Gene **341**: 313-22.

Hooper, C., R. Killick, et al. (2008). "The GSK3 hypothesis of Alzheimer's disease." J Neurochem **104**(6): 1433-9.

Hutton, M., C. L. Lendon, et al. (1998). "Association of missense and 5'-splice-site mutations in tau with the inherited dementia FTDP-17." Nature **393**(6686): 702-5.

Hyman, B. T., J. C. Augustinack, et al. (2005). "Transcriptional and conformational changes of the tau molecule in Alzheimer's disease." Biochim Biophys Acta **1739**(2-3): 150-7.

Ingelsson, M., K. Ramasamy, et al. (2007). "Increase in the relative expression of tau with four microtubule binding repeat regions in frontotemporal lobar degeneration and progressive supranuclear palsy brains." Acta Neuropathol **114**(5): 471-9.

Ingelsson, M., K. Ramasamy, et al. (2007). "Increase in the relative expression of tau with four microtubule binding repeat regions in frontotemporal lobar degeneration and progressive supranuclear palsy brains." Acta Neuropathol (Berl) **114**(5): 471-9.

Iqbal, K., C. Alonso Adel, et al. (2005). "Tau pathology in Alzheimer disease and other tauopathies." Biochim Biophys Acta **1739**(2-3): 198-210.

Kannanayakal, T. J., J. R. Mendell, et al. (2008). "Casein kinase 1 alpha associates with the tau-bearing lesions of inclusion body myositis." Neurosci Lett **431**(2): 141-5.

Kannanayakal, T. J., H. Tao, et al. (2006). "Casein kinase-1 isoforms differentially associate with neurofibrillary and granulovacuolar degeneration lesions." Acta Neuropathol **111**(5): 413-21.

Kelleher, I., C. Garwood, et al. (2007). "Kinase activities increase during the development of tauopathy in htau mice." J Neurochem **103**(6): 2256-67.

Kenessey, A. and S. H. Yen (1993). "The extent of phosphorylation of fetal tau is comparable to that of PHF-tau from Alzheimer paired helical filaments." Brain Res **629**(1): 40-6.

Khan, T. K. and D. L. Alkon (2006). "An internally controlled peripheral biomarker for Alzheimer's disease: Erk1 and Erk2 responses to the inflammatory signal bradykinin." Proc Natl Acad Sci U S A **103**(35): 13203-7.

Khatoon, S., I. Grundke-Iqbal, et al. (1992). "Brain levels of microtubule-associated protein tau are elevated in Alzheimer's disease: a radioimmuno-slot-blot assay for nanograms of the protein." J. Neurochem. **59**(2): 750-753.

King, M. E. (2005). "Can tau filaments be both physiologically beneficial and toxic?" Biochim Biophys Acta **1739**(2-3): 260-7.

King, M. E., V. Ahuja, et al. (1999). "Ligand-dependent tau filament formation: implications for Alzheimer's disease progression." Biochemistry **38**(45): 14851-14859.

King, M. E., T. C. Gamblin, et al. (2000). "Differential assembly of human tau isoforms in the presence of arachidonic acid." J Neurochem **74**(4): 1749-57.

King, M. E., N. Ghoshal, et al. (2001). "Structural analysis of Pick's disease-derived and in vitro-assembled tau filaments." Am. J. Pathol. **158**(4): 1481-1490.

Knippschild, U., S. Wolff, et al. (2005). "The role of the casein kinase 1 (CK1) family in different signaling pathways linked to cancer development." Onkologie **28**(10): 508-14.

Ko, L. W., M. DeTure, et al. (2005). Recent advances in experimental modeling of the assembly of tau filaments. Biochim Biophys Acta. **1739:** 125-39.

Kopke, E., Y. C. Tung, et al. (1993). "Microtubule-associated protein tau. Abnormal phosphorylation of a non-paired helical filament pool in Alzheimer disease." J Biol Chem **268**(32): 24374-84.

Kosik, K. S., L. D. Orecchio, et al. (1989). "Developmentally regulated expression of specific tau sequences." Neuron **2**(4): 1389-97.

Kowalska, A., Z. Jamrozik, et al. (2004). "Progressive supranuclear palsy--parkinsonian disorder with tau pathology." Folia Neuropathol **42**(2): 119-23.

Kristofferson, D., T. L. Karr, et al. (1980). "Dynamics of linear protein polymer disassembly." J Biol Chem **255**(18): 8567-72.

Ksiezak-Reding, H., W. K. Liu, et al. (1992). "Phosphate analysis and dephosphorylation of modified tau associated with paired helical filaments." Brain Res **597**(2): 209-19.

Kuret, J., C. N. Chirita, et al. (2004). "Pathways of tau fibrillizartion." Biochim. Biophys. Acta. In press.

Kuret, J., C. N. Chirita, et al. (2005). "Pathways of tau fibrillization." Biochim Biophys Acta **1739**(2-3): 167-78.

Kuret, J., E. E. Congdon, et al. (2005). "Evaluating triggers and enhancers of tau fibrillization." Microsc Res Tech **67**(3-4): 141-55.

Kuret, J., G. S. Johnson, et al. (1997). "Casein kinase 1 is tightly associated with paired-helical filaments isolated from Alzheimer's disease brain." J Neurochem **69**(6): 2506-15.

Levy, S. F., A. C. Leboeuf, et al. (2005). "Three- and four-repeat tau regulate the dynamic instability of two distinct microtubule subpopulations in qualitatively different manners. Implications for neurodegeneration." J Biol Chem **280**(14): 13520-8.

Li, G., H. Yin, et al. (2004). "Casein kinase 1 delta phosphorylates tau and disrupts its binding to microtubules." J Biol Chem **279**(16): 15938-45.

Liang, Z., F. Liu, et al. (2008). "Decrease of protein phosphatase 2A and its association with accumulation and hyperphosphorylation of tau in Down syndrome." J Alzheimers Dis **13**(3): 295-302.

Liu, F. and C. X. Gong (2008). "Tau exon 10 alternative splicing and tauopathies." Mol Neurodegener **3**: 8.

Liu, R., X. W. Zhou, et al. (2008). "Phosphorylated PP2A (tyrosine 307) is associated with Alzheimer neurofibrillary pathology." J Cell Mol Med **12**(1): 241-57.

Lo, C. L., S. P. Yip, et al. (2007). "One-step rapid reverse transcription-PCR assay for detecting and typing dengue viruses with GC tail and induced fluorescence resonance energy transfer techniques for melting temperature and color multiplexing." Clin Chem **53**(4): 594-9.

Lopes, J. P., C. R. Oliveira, et al. (2007). "Role of cyclin-dependent kinase 5 in the neurodegenerative process triggered by amyloid-Beta and prion peptides: implications for Alzheimer's disease and prion-related encephalopathies." Cell Mol Neurobiol **27**(7): 943-57.

Luo, J., R. He, et al. (2000). "The fluorescent characterization of the polymerized microtubule-associated protein Tau." Int J Biol Macromol **27**(4): 263-8.

Macario, A. J. and E. Conway de Macario (2000). "Stress and molecular chaperones in disease." Int J Clin Lab Res **30**(2): 49-66.

Mandelkow, E. M., G. Drewes, et al. (1992). "Glycogen synthase kinase-3 and the Alzheimer-like state of microtubule-associated protein tau." FEBS Lett **314**(3): 315-21.

McKay, R. M., J. M. Peters, et al. (2001). "The casein kinase I family in Wnt signaling." Dev Biol **235**(2): 388-96.

McKay, R. M., J. M. Peters, et al. (2001). "The casein kinase I family: roles in morphogenesis." Dev Biol **235**(2): 378-87.

Meldgaard, M., C. Fenger, et al. (2006). "Validation of two reference genes for mRNA level studies of murine disease models in neurobiology." J Neurosci Methods **156**(1-2): 101-10.

Meng, Q. J., L. Logunova, et al. (2008). "Setting clock speed in mammals: the CK1 epsilon tau mutation in mice accelerates circadian pacemakers by selectively destabilizing PERIOD proteins." Neuron **58**(1): 78-88.

Myers, A. J., A. M. Pittman, et al. (2006). "The MAPT H1c risk haplotype is associated with increased expression of tau and especially of 4 repeat containing transcripts." Neurobiol Dis.

Necula, M., C. N. Chirita, et al. (2003). "Rapid anionic micelle-mediated alpha-synuclein fibrillization in vitro." J Biol Chem **278**(47): 46674-80.

Necula, M., C. N. Chirita, et al. (2005). "Cyanine dye N744 inhibits tau fibrillization by blocking filament extension: implications for the treatment of tauopathic neurodegenerative diseases." Biochemistry **44**(30): 10227-37.

Necula, M. and J. Kuret (2004). "Electron microscopy as a quantitative method for investigating tau fibrillization." Anal Biochem **329**(2): 238-46.

Necula, M. and J. Kuret (2004). "Pseudophosphorylation and glycation of tau protein enhance but do not trigger fibrillization in vitro." J Biol Chem **279**(48): 49694-703.

Necula, M. and J. Kuret (2004a). "Electron Microscopy as a Quantitative Method for Investigating tau Fibrillization." Anal. Biochem. **329**: 238-246.

Necula, M. and J. Kuret (2004b). "Static Laser Light Scattering Assay for Surfactant - induced Protein Fibrillization." Anal. Biochem. In press.

Paglini, G., L. Peris, et al. (2000). "Tau protein function in axonal formation." Neurochem Res **25**(1): 37-42.

Preece, P. and N. J. Cairns (2003). "Quantifying mRNA in postmortem human brain: influence of gender, age at death, postmortem interval, brain pH, agonal state and inter-lobe mRNA variance." Brain Res Mol Brain Res **118**(1-2): 60-71.

Reiser, G. and H. G. Bernstein (2002). "Neurons and plaques of Alzheimer's disease patients highly express the neuronal membrane docking protein p42IP4/centaurin alpha." Neuroreport **13**(18): 2417-9.

Roder, H. M., P. A. Eden, et al. (1993). "Brain protein kinase PK40erk converts TAU into a PHF-like form as found in Alzheimer's disease." Biochem Biophys Res Commun **193**(2): 639-47.

Rubinsztein, D. C. and J. Carmichael (2003). "Huntington's disease: molecular basis of neurodegeneration." Expert Rev Mol Med **5**(20): 1-21.

Samsonov, A., J. Z. Yu, et al. (2004). "Tau interaction with microtubules in vivo." J Cell Sci **117**(Pt 25): 6129-41.

Santhosh, S. R., M. M. Parida, et al. (2007). "Development and evaluation of SYBR Green I-based one-step real-time RT-PCR assay for detection and quantification of Chikungunya virus." J Clin Virol **39**(3): 188-93.

Schindowski, K., K. Belarbi, et al. (2008). "Neurogenesis and cell cycle-reactivated neuronal death during pathogenic tau aggregation." Genes Brain Behav **7 Suppl 1**: 92-100.

Schwab C, S. J., Akiyama H, McGeer EG, McGeer PL. (1995). "Relationship of amyloid beta/A4 protein to the neurofibrillary tangles in Guamanian parkinsonism-dementia." Acta Neuropathol. (Berl.) **90**(3): 287-298.

Selkoe, D. J. (2004). "Cell biology of protein misfolding: the examples of Alzheimer's and Parkinson's diseases." Nat Cell Biol **6**(11): 1054-61.

Shi, J., T. Zhang, et al. (2008). "Increased dosage of Dyrk1A alters ASF-regulated alternative splicing of tau in down syndrome." J Biol Chem.

Siebert, A., A. Neumann, et al. (2002). "A non-dechlorinating strain of Dehalospirillum multivorans: evidence for a key role of the corrinoid cofactor in the synthesis of an active tetrachloroethene dehalogenase." Arch Microbiol **178**(6): 443-9.

Singleton, A., A. Myers, et al. (2004). "The law of mass action applied to neurodegenerative disease: a hypothesis concerning the etiology and pathogenesis of complex diseases." Hum Mol Genet **13 Spec No 1**: R123-6.
Sisodia, S. S. and R. E. Tanzi (2007). Alzheimer's disease : advances in genetics, molecular and cellular biology. New York, Springer.

Spillantini, M. G., J. C. Van Swieten, et al. (2000). "Tau gene mutations in frontotemporal dementia and parkinsonism linked to chromosome 17 (FTDP-17)." Neurogenetics **2**(4): 193-205.

Stoothoff, W. H. and G. V. Johnson (2005). "Tau phosphorylation: physiological and pathological consequences." Biochim Biophys Acta **1739**(2-3): 280-97.

Takanashi, M., H. Mori, et al. (2002). "Expression patterns of tau mRNA isoforms correlate with susceptible lesions in progressive supranuclear palsy and corticobasal degeneration." Brain Res Mol Brain Res **104**(2): 210-9.

Takeda, A., N. Arai, et al. (1997). "Tau immunoreactivity in glial cytoplasmic inclusions in multiple system atrophy." Neurosci Lett **234**(1): 63-6.

Takuma, H., S. Arawaka, et al. (2003). "Isoforms changes of tau protein during development in various species." Brain Res Dev Brain Res **142**(2): 121-7.

Timm, T., D. Matenia, et al. (2006). "Signaling from MARK to tau: regulation, cytoskeletal crosstalk, and pathological phosphorylation." Neurodegener Dis **3**(4-5): 207-17.

Uversky, V. N. (2002). "What does it mean to be natively unfolded?" Eur J Biochem **269**(1): 2-12.

Uversky, V. N., J. R. Gillespie, et al. (2000). "Why are "natively unfolded" proteins unstructured under physiologic conditions?" Proteins **41**(3): 415-27.

Uversky, V. N., C. J. Oldfield, et al. (2008). "Intrinsically disordered proteins in human diseases: introducing the D2 concept." Annu Rev Biophys **37**: 215-46.

van Swieten, J. C., I. F. Bronner, et al. (2007). "The DeltaK280 mutation in MAP tau favors exon 10 skipping in vivo." J Neuropathol Exp Neurol **66**(1): 17-25.

Vielhaber, E. and D. M. Virshup (2001). "Casein kinase I: from obscurity to center stage." IUBMB Life **51**(2): 73-8.

von Bergen M, B. S., Biernat J, Mandelkow EM, Mandelkow E. (2005). "Tau aggregation is driven by a transition from random coil to beta sheet structure." Biochim Biophys Acta **1739**(2-3): 158-66.

Walter, J., A. Schindzielorz, et al. (2000). "Phosphorylation of the beta-amyloid precursor protein at the cell surface by ectocasein kinases 1 and 2." J Biol Chem **275**(31): 23523-9.

Wang, J., X. Wang, et al. (2002). "In vitro analysis of tau phosphorylation sites and its biological activity." Chin Med Sci J **17**(1): 13-6.

Wang, J. Z., I. Grundke-Iqbal, et al. (2007). "Kinases and phosphatases and tau sites involved in Alzheimer neurofibrillary degeneration." Eur J Neurosci **25**(1): 59-68.

Wang, Y., Q. Wang, et al. (2002). "[Detection of level and mutation of neurofilament mRNA in Alzheimer's disease]." Zhonghua Yi Xue Za Zhi **82**(8): 519-22.

Wilson, D. M. and L. I. Binder (1997). "Free fatty acids stimulate the polymerization of tau and amyloid beta peptides. In vitro evidence for a common effector of pathogenesis in Alzheimer's disease." Am J Pathol **150**(6): 2181-95.

Wilson, D. M. and L. I. Binder (1997). "Free fatty acids stimulate the polymerization of tau and amyloid beta peptides. In vitro evidence for a common effector of pathogenesis in Alzheimer's disease." Am. J. Pathol. **150**(6): 2181-2195.

Wright, P. E. and H. J. Dyson (1999). "Intrinsically unstructured proteins: re-assessing the protein structure-function paradigm." J Mol Biol **293**(2): 321-31.

Wszolek, Z. K., Y. Tsuboi, et al. (2006). "Frontotemporal dementia and parkinsonism linked to chromosome 17 (FTDP-17)." Orphanet J Rare Dis **1**: 30.

Yasojima, K., E. G. McGeer, et al. (1999). "Tangled areas of Alzheimer brain have upregulated levels of exon 10 containing tau mRNA." Brain Res **831**(1-2): 301-5.

Yin, H. and J. Kuret (2006). "C-terminal truncation modulates both nucleation and extension phases of tau fibrillization." FEBS Lett **580**(1): 211-5.

Yuzwa, S. A., M. S. Macauley, et al. (2008). "A potent mechanism-inspired O-GlcNAcase inhibitor that blocks phosphorylation of tau in vivo." Nat Chem Biol **4**(8): 483-90.